Bioorganic Chemistry 104 (2020) 104207

Contents lists available at ScienceDirect

Bioorganic Chemistry

journal homepage: www.elsevier.com/locate/bioorg

Coumarin-chalcone hybrids targeting insulin receptor: Design, synthesis, anti-diabetic activity, and molecular docking

Sathish Kumar Konidala[a,c], Vijay Kotra[b], Ravi Chandra Sekhara Reddy Danduga[a], Phani Kumar Kola[a,*]

[a] University College of Pharmaceutical Sciences, Acharya Nagarjuna University, Nagarjuna Nagar, Guntur, A.P. 522510, India
[b] Faculty of Pharmacy, Quest International University Perak (QIUP), Ipoh, Malaysia
[c] School of Pharmaceutical Sciences, Vignan's Foundation for Science, Technology, and Research, Guntur, Andhra Pradesh 522213, India

ARTICLE INFO

Keywords:
Coumarin-chalcone
Hybrids
Streptozocin + Nicotinamide
Anti-diabetic
Histopathology

ABSTRACT

Four series of thirteen new coumarin-chalcone hybrids (DPCU 1–13, DPCT 1–13, DCCU 1–13 and DCCT 1–13) were designed and synthesized using Biginelli synthesis, Pechmann condensation, Acetylation, and Claisen-Schmidt reactions. Synthesized compounds were tested for insulin receptor *in silico* docking studies (PDB ID: 1IR3); DCCU 13 and DCCT 13 derivatives received the lowest docking score; Streptozocin (STZ) and Nicotinamide (NA) induced type II diabetes was tested for their anti-diabetic activity in rats. *In vivo* tests suggested that fasting blood glucose levels of animals treated with DCCU 13 (30 mg/kg body weight) and DCCT 13 (30 mg/kg body weight) were significantly and moderately suppressed, respectively, relative to fasting blood glucose levels of diabetic control animals. Similarly, therapy with DCCU 13 and DCCT 13 attenuated oxidative stress parameters such as lipid peroxidation (MDA), superoxide dismutase (SOD) and increased the glutathione (GSH) in the liver and pancreas in a dose-dependent manner. In comparison, therapy with DCCU 13 (30 mg/kg body weight) mitigated alterations in the histological architecture of the liver and pancreatic tissue. These results indicated that the hybrids DUUC 13 and DCCT 13 at 30 mg/kg had an anti-hyperglycemic and anti-oxidant impact on STZ + NA mediated type II diabetes in rats. Further detailed work could be required to determine the precise mode of action of the anti-diabetic behavior of hybrids.

1. Introduction

Diabetes mellitus (DM) is a persistent metabolic condition marked by long-term rises in blood glucose rates, elevated serum triglycerides, polyuria, polyphagia and polydipsia [1,2]. Type II diabetes mellitus is one type of DM found in more than 90 percent of cases of DM and could be attributed to obesity, overweight and lack of physical activity, marked by pancreatic insulin release, when the body has not been trained to utilize insulin developed for glucose transfer, and the emergence of insulin resistance contributes to an increase of blood glucose or hyperglycemia [2]. Long-term sensitivity to medications and changes in blood glucose rates contributes to comorbidity; nephropathy, retinopathy, neuropathy, atherosclerosis, myocardial infarction and stroke [3].

Currently available oral anti-hyperglycemic agents display tolerance and adverse reactions such as hypoglycemia, gastrointestinal disorders, hypersensitivity reactions, weight gain and harm to main organs [4]. If this persists, the number of diabetic cases is projected to reach as large as 366 million in 2030 from 171 million in 2000, so new medicines that can successfully treat DM problems as current drugs need to be developed [5]. As a consequence, early work on the production of anti-diabetic drugs centered on insulin-sensitizing agents.

Heterocyclic molecules, coumarin, chalcones, and their derivatives are accessible from natural and synthetic sources and have gained the greatest interest in contemporary drug production and research attributable to their wide variety of pharmacological activities. Drug research utilizes various methods to the production of new drugs; molecular hybridization is one of the latest strategies that help the chemical fusion of two or more pharmacophores to boost or enhance or maximize different pharmacological activity [6].

The current drug production approach uses a robust, *in silico* methodology to construct lead molecules for their pharmacological activities by growing manufacturing costs and time [7]. The development of anti-diabetic drugs by *in silico* technique involves the molecules

* Corresponding author at: Department of Pharmacology, University College of Pharmaceutical Sciences, Acharya Nagarjuna University, Nagarjuna Nagar, Guntur, A.P. 522510, India.
E-mail address: drphanikumarkola@gmail.com (P.K. Kola).

https://doi.org/10.1016/j.bioorg.2020.104207
Received 12 April 2020; Received in revised form 25 July 2020; Accepted 24 August 2020
Available online 28 August 2020

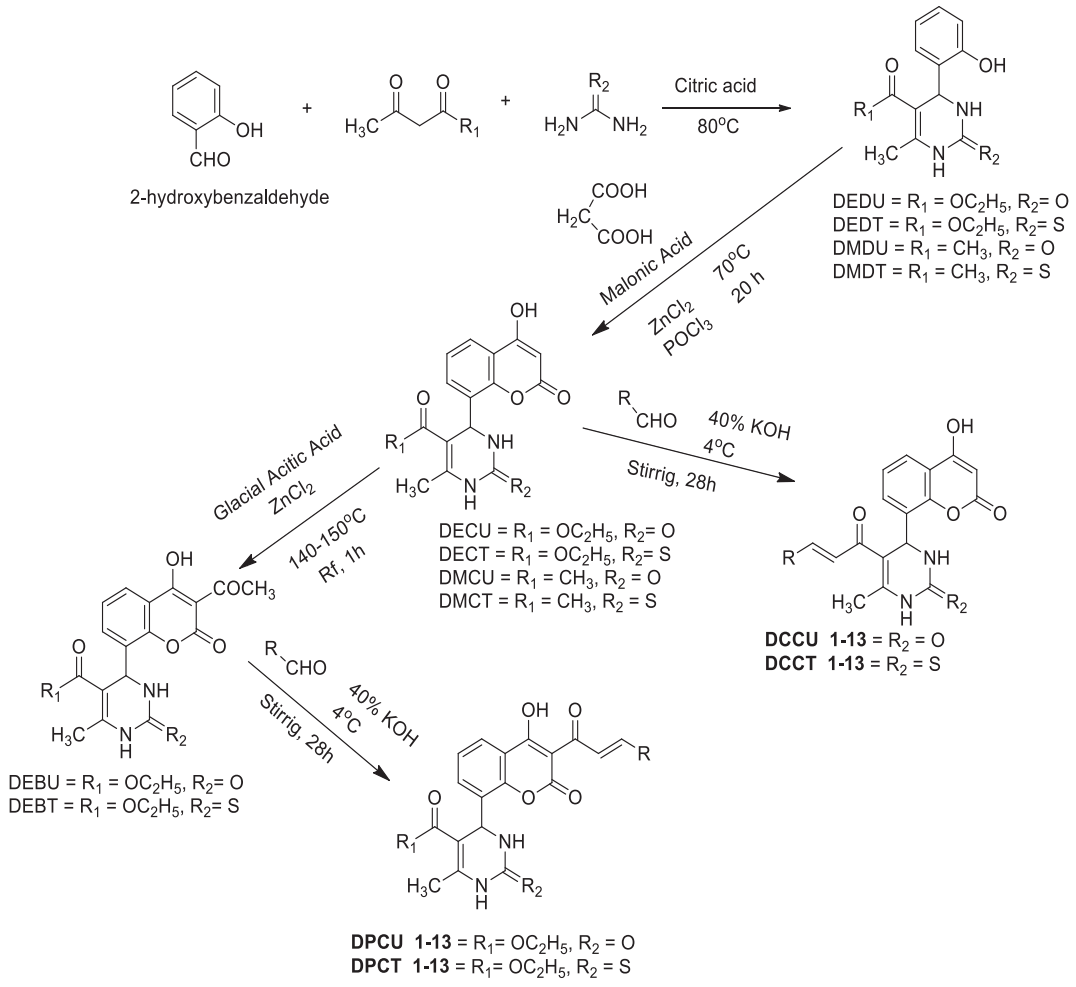

Scheme 1.

designed to be evaluated for one or more diabetic-related biological targets such as insulin receptor, dipeptidyl peptidase IV (DPP IV), glycogen synthase kinase 3 beta (GSK-3beta), Fructose 1,6-bisphosphatase, Glycogen phosphorylase, (GLP-1), α glucosidase, Protein Tyrosine Phosphatase 1-Beta (PTP-1B), G protein-coupled receptors, Sodium-glucose co-transporter type 2, free fatty acid receptors 1 (FFAR1), Glucokinase, Peroxisome Proliferator-activated Receptor (PPAR) –γ, Aldose reductase (AR), etc. [8].

The coumarins are the main grouping of 1-benzopiran derivatives. They are primarily found in higher plants. Some natural coumarins are oxygenated at C-7; umbelliferone (7-hydroxycoumarin) is thought to be the structural and biogenic parent of more heavily oxygenated coumarins [9]. Coumarin and its compounds may be synthesized using various processes, such as Pechmann [10], Knoevenagel [11], Perkin [12], Friedel-Crafts [13], Reformatsky [14] and Wittig [15] reactions. Coumarin and its derivatives possess anticoagulant [16] Antimicrobial [17,18], antioxidant [19], anti-inflammatory [20], anticancer [21], anti HIV [22], antituberculosis [23], anti-influenza [24], anti-Alzheimer [25], antiviral [26], antihyperlipidemic [27], Antihypertensive [28], Anticonvulsant [29], Antiadipogenic [30], Cytochrome P450 Inhibiting [31], Neuroprotective [32], analgesic [33], antimalarial [34], anti-tumor [35–37], antipsychotics [38,39], anti-diabetic [39,40], xanthine oxidase inhibitors [41] activities and are also used for the treatment of multiple sclerosis [42].

Flavonoids and isoflavonoids are the major precursors in biosynthesis of chalcones as secondary metabolites in terrestrial plants. Chalcones (1,3-diaryl-2-propane-1-ones) is one of the main groups of natural products, commonly found in berries, herbs, spices, tea and soy-based foods [43]. Chemically chalcones comprise an open-chain flavonoid moiety, the fundamental form of which consists of two aromatic

rings connected by three carbons, the β-unsaturated carbonyl system [44]. Chalcones and its derivatives can be synthesized using several approaches, but the Claisen-Schmidt condensation always retains a high position. The best approach for chalcone synthesis is the traditional Claisen-Schmidt [45]. Many renowned techniques include the Suzuki reaction [46], Friedel-Crafts acylation [47] with cinnamoyl chloride, Allan-Robinson Condensation [48], Direct Cross-coupling Reaction [49], Microwave Irradiation [50], Julia-Kocienski Olefination [51], and Grinding Technique [52]. Chalcones have been reported to possess many useful biological properties including antimicrobial [53], anti-inflammatory [54], anticancer [55], anti-HIV [56], antioxidant [57], Anticoagulant [58], Antituberculosis [59], antipsychotic [60] and antimalarial [61] activities.

Many research groups reported the potential effects of coumarin-chalcone hybrids like anti-microbial [62,63], anti-cancer [64,65], anti-malarial [66,67], anti-oxidant [68,69], anti-tubercular [70,71], and anti-inflammatory [72]. Even though the coumarin and chalcone and their derivatives obtained from natural origin, synthetic coumarin-chalcone derivatives with structural modifications may be adapted for the development of potent biologically active molecules. Hence, the present study was aimed to evaluate the anti-diabetic activity of synthesized coumarin-chalcone hybrids against Streptozotocin + Nicotinamide induced diabetes in rats.

2. Experimental

The chemicals used for the synthesis were laboratory-grade, which were procured from Loba Chemie Pvt. Ltd. (Mumbai, India), SD Fine Chemicals Pvt. Ltd. (Mumbai, India) Fisher Scientific (Mumbai, India), Merck Pvt. Ltd. (Mumbai, India), Avra Synthesis Pvt. Ltd. (Hyd. India). Streptozotocin, Nicotinamide, and 2,2-diphenyl-1-picrylhydrazyl (DPPH) reagent were purchased from Sisco Research Laboratories Pvt. Ltd. (Taloja, India); Pyrogallol and Thiobarbituric acid were procured from Merck Pvt. Ltd. (Mumbai, India). All the chemicals were of commercial grade and used without further purification.

In silico molecular docking was conducted using Chem Office 2016 and VLife MDS 4.6. Control D Glucose meter and blood glucose monitor strip kits were purchased from Haiden technology Pvt. Ltd. (New Delhi, India, USA). The melting points of the synthesized compounds were determined using open capillary tubes by the Dalal Melting Point Apparatus. Bruker FTIR spectrophotometer was used to capture infrared spectra using the KBr Pellet method. ^{1}H NMR and ^{13}C NMR spectra were determined using the Bruker-NMR 400 MHz spectrometer at Laila Impex, Vijayawada. Mass spectra were analyzed with Shimadzu GC–MS QP 5000 mass spectrometer in Laila Impex, Vijayawada. The success of organic reactions and the quality of reaction end products was confirmed by Thin Layer Chromatography on TLC silica gel F_{254} aluminium plates (E. Merck, Germany), utilizing acetone and ethyl acetate as a mobile process, the spots are visualized with UV chamber and iodine vapours.

2.1. Scheme

See Scheme 1.

2.2. Procedure for synthesis of coumarin-chalcone hybrids

Four series of coumarin-chalcone derivatives (DPCU 1–13, DPCT 1–13, DCCU 1–13, and DCCT 1–13) were designed and synthesised Biginelli synthesis [73], Pechmann condensation [74], Acetylation [75] and Claisen- Schmidt reactions [76] with good yield (54–78%) as described in experimental procedures. Intermediate products DEDU, DEDT, DMDU, and DMDT were also synthesized by reacting Salicylaldehyde, Ethylacetoacetate or Acetylacetone, Urea or Thiourea, and Citric acid and the products DECU, DECT, DMCU, and DMCT were synthesized by introducing corresponding first-stage malonic acid products to the pre-heated mixture of phosphorus oxychloride and anhydrous zinc chloride at 70 °C for 20 h. Final derivatives (DCCU 1–13 and DCCT 1–13) were synthesized by reacting DMCU and DMCT with different aromatic aldehydes in the presence of sodium hydroxide, while DEBU and DEBT products were synthesized by acetylation of DECU and DECT with glacial acetic acid in the presence of zinc chloride under reflux at 140–150 0C at about 1 h. Final derivatives (DPCU 1–13 and DPCT 1–13) were synthesized by reacting DMBU and DMBT with different aromatic aldehydes in the presence of Sodium hydroxide. Completion of synthetic reactions and purity of end products of reactions were confirmed by Thin Layer Chromatography on TLC silica gel F254 aluminium plates (E. Merck, Germany), using acetone and ethyl acetate as mobile spots are visualized with UV chamber and iodine vapours.

2.3. Docking studies

The Docking study was conducted to test *in silico* anti-diabetic action of synthesized derivatives DPCU1-13, DPCT 1–13, DCCU 1–13 and DCCT 1–13 against insulin receptor (1IR3) using VLife MDS 4.6 software. The ligands were prepared by drawing 2D structures, translating to 3D structures, optimized to minimize energy and conformers were generated using the VLife engine tools. The X- crystal structure of the insulin receptor (1IR3) was obtained from the rcsb.com/pdb database. The protein crystal structure was corrected by the elimination of water molecules, the introduction of hydrogens. The co-crystal ligand (ANP) was recognised, extracted from protein amino acid sequence and the protein structure and co-crystal ligand (which should be used as reference ligand) were saved in.mol2 format. The protein structure was validated by checking criss cross residues, local geometry, Ramachandran plot by VLife MDS Biopredicta tools and the protein was optimized by minimizing the energy through force field minimization tool. The insulin receptor docking procedure through Vlife MDS software was validated by re-docking the extracted co-crystal ligand ANP. The grid docking was conducted using GRIP docking under the batch docking method of the Biopredicta module. The interpretation of the outcome was based on the score obtained by the ligand conformers. The conformer with the lowest score will be the one with strong binding energy to the active protein site. Interactions between ligand and protein may be explored by selecting various scoring options such as hydrogen bonding, hydrophobic interactions Pi-stacking, van der Waals force, etc. by examination of interactions tool in the Biopredicta module.

2.4. Experimental animals

Albino Wister female (9) and male (42) rats weight about 150 to 200 gm were procured from Sainath Agencies Laboratory animal suppliers Hyderabad. The animals were handled according to the protocol approved by the Institutional Animal ethical committee (IAEC), University College of Pharmaceutical Sciences, Acharya Nagarjuna University, Guntur, A.P., India, under CPCSEA, New Delhi bearing the number ANUCPS/IAEC/AH/P13/2019. Animals were acclimatized in 12 h dark and light cycles at room temperature, the humidity of 55 ± 5% and free access to feed and water for about one week before starting the experiment.

2.5. Acute toxicity studies

Acute oral toxicity studies were performed as per the OECD (Economic Cooperation and Development Organization) part 423 of the Guidelines [77]. Albino Wistar female rats (9) Weigh between 150 and 200 gm, grouped three in each and fasted overnight. The test hybrids DCCU 8 and DCCU 13 solutions of 300 mg/kg body weight of animal dose were prepared in 0.5% carboxy methylcellulose (CMC) and were administered orally to the animals, then the animals were observed for

any changes in skin colour, changes in eyes, salivation, diarrhoea, tremors, convulsions, sleep, and coma at every 1 h/24 h and for every 24 h /14 days after treatment.

2.6. In vivo anti-diabetic assay

2.6.1. Induction of diabetes mellitus

Type II diabetes mellitus was induced by a single intraperitoneal (i.p.) dose of 60 mg/kg of freshly prepared Streptozotocin (STZ) in citrate buffer (pH 4.5) in male rats after 30 min of intraperitoneal (i.p.) administration of 110 mg/kg of Nicotinamide (NA) in regular saline solution. The hypoglycemic shock triggered by Streptozotocin was stopped by the injection of 5% glucose solution to the animals for 24 h following treatment with STZ [78]. Blood samples were collected from the tail tips of fasted animals after 3 to 5 days and the blood glucose level (BGL) was measured by the Control D glucose control system. Animals having fasted BGL over 180 mg/dL were considered to be diabetic animals in the experiment. Common animals without any medication of BGL less than 100 mg/dL were included in the control group.

2.6.2. Experimental design

The animals (42) were grouped into seven classes, each of which had six animals, fasting overnight prior to the treatment. Animal groups were administered twice every day for 7 days with equivalent doses of less than 1 mL of 0.5 percent carboxymethyl cellulose (CMC) as follows: Group I (Normal control): Normal healthy male rats treated with 0.5% CMC orally, Group II (Diabetic Control): Diabetic rats treated with 0.5% CMC orally, Group III (STD): Diabetic rats treated with 100 mg/kg dose of Metformin in 0.5% CMC orally, Group IV (DCCU 13 Low): Diabetic rats treated with 15 mg/kg b.d. dose of DCCU 13 dissolved in 0.5% CMC orally, Group V (DCCU 13 High): Diabetic rats treated with 30 mg/kg b.d. dose of DCCU 13 dissolved in 0.5% CMC orally, Group VI (DCCT 13 Low): Diabetic rats treated with 15 mg/kg b.d. dose of DCCT 13 dissolved in 0.5% CMC orally, Group VII (DCCT 13 High): Diabetic rats treated with 30 mg/kg b.d. dose of DCCT 13 dissolved in 0.5% CMC orally. Fasting blood tests were conducted prior to treatment and at the end of the 0th day, 1st day, 3rd day and 7th day of treatment to evaluate fasting blood glucose level and body weights on the same days. On the last day of the experimental protocol (7th), the animals were sacrificed and isolated pancreas and liver tissues were subjected for determination of oxidative stress-related parameters such as MDA, SOD, and GSH. Apart from pancreas and liver tissues were fixed in 4% formalin solution and sent for histopathological investigation.

2.7. Determination of oxidative stress-related enzymes in the pancreas and liver

2.7.1. Lipid peroxides (MDA)

Malondialdehyde (MDA) was determined by spectrophotometry [79] using the thiobarbituric acid (TBA). Tissue was homogenized in 0.1 M phosphate buffer using a homogenizer, about 0.1 mL of tissue homogenate was added to 1 mL of 10% trichloroacetic acid and 1 mL of 0.67% Thiobarbituric acid, boil the resulting solution at 90 °C for around 30 min, cool the contents and calculate the absorbance at 532 nm in the spectrophotometer using the same without homogenizing as null. The concentration of MDA was measured using a molar extinction coefficient of 156,000 M^{-1} cm^{-1} expressed in nM/gm of wet tissue.

2.7.2. Superoxide dismutase (SOD)

Superoxide dismutase (SOD) was determined by the spectrophotometric method [80,81] utilizing Pyrogallol as an autoxidizing agent. Freshly prepared 0.5 mL of 0.2 mM Pyrogallol in 0.01 N HCl was immediately added to tissue 0.5 mL of homogenate in 2 mL of 50 mM Tris-HCl buffer with pH 8.2. The change in the rate of absorbance was measured at 420 nm for about 2 min using the same solution except the homogenate as the control. The increase in absorbance with time due to Pyrogallol autoxidation is decreased with increased SOD concentration is high in samples. The SOD values were represented as U/gm wet tissue.

2.7.3. Reduced glutathione (GSH)

Reduced glutathione (GSH) was measured in homogenized tissue samples in cold SSA (5% w/v in distilled water) with a homogenizer, then add 0.5 mL of the homogenate to 0.5 mL of 10% trichloroacetic acid (TCA), centrifuge at 14,000 RPM for 15 min (4 °C), the supernatant was collected and treated with 3 mL of 0.2 M phosphate buffer and 0.5 mL of 10 mM 5,5′-dithiobis (2-nitrobenzoic acid) (DTNB), finally measured the absorbance at 412 nm in a spectrophotometer using 4 mL of 0.2 M phosphate buffer and 0.5 mL of 10 mM 5,5′-dithiobis (2-nitrobenzoic acid) (DTNB), as blank. The concentration of reduced glutathione was calculated using the molar extinction coefficient of 13,600 M^{-1} cm^{-1} and expressed in μM/gm of wet tissue [82,83].

2.8. Histopathology

A portion of isolated tissues of the pancreas and liver of animal groups were fixed in 10% formalin solution for about 48 h [79] and were dehydrated, embedded in paraffin wax, sections were cut, stained with hematoxylin-eosin and fixed on slides. The slides were observed under an electronic microscope for histopathological changes.

2.9. Statistical analysis

All the data were collected in triplicate and represented as mean ± standard error of the mean (SEM). The interpretation was done through one-way ANOVA followed by Tukey's post hoc test by Graph pad prism 5.0v. The significance was represented as ***$p \leq 0.001$, **$p \leq 0.01$, *$p \leq 0.5$ and ns = non-significant.

3. Results

3.1. Chemistry

Four series of new coumarin-chalcone hybrids (DPCU 1–13, DPCT 1–13, DCCU 1–13 and DCCT 1–13) of using salicylaldehyde, ethyl acetoacetate, urea (DPCU 1–13) or thiourea (DPCT 1–13) as starting materials through Biginelli synthesis, Pechmann condensation, Acetylation, and Claisen-Schmidt reactions, and using salicylaldehyde, acetyl acetate, urea (DCCU 1–13)/thiourea (DCCT 1–13) as starting materials through Biginelli synthesis, Pechmann condensation, and Claisen-Schmidt reactions, the completion of reactions were monitored by Thin layer chromatography (TLC) and final compounds were purified by recrystallization from ethyl alcohol.

The cyclo condensation phenomena occur in Biginelli synthesis step by reaction of activated salicylaldehyde under acidic medium with urea or the thiourea those act as nucleophile to form heminal species which liberates water molecule to form as *N*-acyliminium cation that further reacts with the α-carbon atom of the β-keto ester to form hexahydropyrimidine and liberates water molecule to form the stable dihydropyrimidine product. Pechmann condensation step includes the transesterification, keto-enol tautomerization, nucleophilic addition, rearomatisation and dehydration of phenol group with malonic acid under the strongly acidic conditions leads to the formation of 4-hydroxy coumarin product. Acetylation at the 3rd position of the coumarin ring occurred by electrophilic aromatic substitution with glacial acetic acid. The final step Claisen Schmidt condensation includes the aldol reaction, i.e. nucleophilic addition of ketone enolate to the aldehyde and dehydration (removal of a water molecule) in the presence of strong alkali leads to the formation of end products.

The end product of Biginelli synthesis under citric acid (86.46%)

and Pechmann condensation under the malonic acid presence of phosphorous oxychloride and zinc chloride mixture gives a high product yield ((82.45%) than the Biginelli synthesis under sulphuric acid (42.72%) and Pechmann condensation under the excess amount of concentrated sulphuric acid (25.17%).

The title hybrids chemical structures were confirmed through FTIR, ^{1}H NMR, ^{13}C NMR spectroscopy and Mass Spectrometry techniques by observing characteristic peaks at around 3400–3450 cm^{-1} (OH), 3150–3250 cm^{-1} (NH), 1700–1750 cm^{-1} (C═O), and 1250–1300 cm^{-1} (C−O−C) for DPCU 1–13, missing of 1700–1750 cm^{-1} (C═O) for DPCT 1–13 series, missing of 1250–1300 cm^{-1} (C−O−C) for DCCU 1–13 series and missing of 1250–1300 cm^{-1} (C−O−C), and 1700–1750 cm^{-1} (C═O) for DCCT 1–13 series in IR spectra, peaks at around 5 δ value (C−C, Aromatic), 6 δ value (NH), 7.7 δ value (C═C), and 9.5 δ value (OH) in ^{1}H NMR spectra, and the molecular ion peak at corresponding e/z value as M^{+1} or M^{+2} for respective derivatives.

Ethyl 4-(3-cinnamoyl-4-hydroxy-2-oxo-2H-chromen-8-yl)-6-methyl-2-oxo-1,2,3,4-tetrahydropyrimidine-5-carboxylate (DPCU 1): Yellow solid; yield 61.42%; m.p. 149–151 °C; IR (KBr, cm^{-1}): v 3482(O−H), 3270(N−H), 2920 (C−H Ar), 2851(C−H), 1724(C═O), 1671(C═O), 1600, 1474 (C═C), 1281 (C−O−C); ^{1}H NMR (400 MHz, DMSO-d_6, δ/ppm): 1.41(t, 3H, CH), 1.95(s, 3H, CH), 4.73(q, 2H, CH), 5.21(s, H, CH−Ar), 6.19(s, 2H, NH), 6.93–7.34 (m, 8H, Ar), 7.78(d, 2H, HC═CH), 11.23 (s, H, OH). ^{13}C NMR (100 MHz, DMSO-d_6) δ/ppm: 16.3 (CH_3), 18.5(CH_3), 41.2(CH, Ar), 59.7(CH_2), 99.3, 106.2, 117.7, 124.2, 125.5, 126.1, 128.6, 135.3, 148.5, (Ar−C), 147.2 (C−N), 150.5 (C═O), 152.8 (C═C), 159.4 (C═O), 167.9 (C═O), 179.2(C−OH), 183.1 (C═O). MS (*m/z*, (relative abundance, %)): 475 (M^{+}, 9.6), 402 (36), 273 (100), 162 (49), 132 (27), 74(16).

Ethyl-4-(4-hydroxy-3-(3-(4-methoxyphenyl)acryloyl)-2-oxo-2H-chromen-8-yl)-6-methyl-2-oxo-1,2,3,4-tetrahydropyrimidine-5-carboxylate (DPCU 2): Dark red solid; yield 59.24%; m.p. 195–197 °C; IR (KBr, cm^{-1}): v 3399(O−H), 3249(N−H), 2920 (C−H Ar), 2851 (C−H), 1735(C═O), 1669(C═O), 1601, 1474 (C═C), 1251 (C−O−C), 831 (p-sub); ^{1}H NMR (400 MHz, DMSO-d_6, δ/ppm): 1.27(t, 3H, CH), 1.64(s, 3H, CH), 3. 54(s, 3H, OH) 4.48(q, 2H, CH), 5.11(s, H, CH−Ar), 6.07(s, 2H, NH), 6.73–7.23 (m, 7H, Ar), 7.56(d, 2H, C = CH), 11.46 (s, H, OH). ^{13}C NMR (100 MHz, DMSO-d_6) δ/ppm: 15.9 (CH_3), 17.9 (CH_3), 40.6(C−CH), 56.6(CH_3), 62.3 (CH_2), 97.5, 105.7, 114.7, 117.2, 123.3, 124.4, 125.3, 126.7, 128.4, 147.2, 150.1, (Ar−C), 152.4 (C═O), 152.8 (C═O),159.4 (C═O),166.4 (C═O), 179.6(C = OH), 182.4 (C═O). MS (*m/z*, (relative abundance, %)): 505 (M^{+1}, 10.5), 432 (100), 322 (31), 184 (17), 74 (44).

Ethyl-4-(4-hydroxy-2-oxo-3-(5-phenylpenta-2,4-dienoyl)-2H-chromen-8-yl)-6-methyl-2-oxo-1,2,3,4-tetrahydropyrimidine-5-carboxylate (DPCU 3): Yellow solid; yield 64.37%; m.p. 167–169 °C): IR (KBr, cm^{-1}): v 3473(O−H), 3236(N−H), 2921 (C−H Ar), 2851 (C−H), 1749(C═O), 1675(C═O), 1601, 1474 (C═C), 1282 (C−O); ^{1}H NMR (400 MHz, DMSO-d_6, δ/ppm): 1. 62 (t, 3H, CH), 2.57(s, 3H, CH), 4.25(q, 2H, CH), 5.14 (s, H, CH−Ar), 6.12 (s, 2H, NH), 6.65–7.57 (m, 12H, Ar), 9.45 (s, H, OH). ^{13}C NMR (100 MHz, DMSO-d_6) δ/ppm: 15.2 (CH_3), 17.6 (CH_3), 41.4(C−CH), 62.5(CH_2), 96.8, 106.8, 117.5, 124.3, 125.9, 126.7, 128.4, 128.9, 135.9, 146.8, 148.3(Ar−C), 150.4 (C═O), 151.1 (C═C), 158.8(C═O), 166.9 (C═O), 179.4 (C−OH), 183.2 (C═O). MS (*m/z*, (relative abundance, %)): 501 (M^{+1}, 9.2), 428 (100), 318 (27), 184 (38), 74(32).

Ethyl 4- (4-hydroxy-3-(3-(2-nitrophenyl) acryloyl)-2-oxo-2H-chromen-8-yl)-6-methyl-2-oxo-1,2,3,4-tetrahydropyrimidine-5-carboxylate (DPCU 4). Green solid; yield 57.37%; m.p. 210–212 °C; IR (KBr, cm^{-1}): v 3348(O−H), 3257(N−H), 2922 (C−H Ar), 2851 (C−H), 1732(C═O), 1668(C═O), 1610, 1474 (C═C), 1574, 1391 (N−O), 1257 (C−O), 868 (o-sub); ^{1}H NMR (400 MHz, DMSO-d_6, δ/ppm): 1.53(t, 3H, CH), 2.11(s, 3H, CH), 4.17 (q, 2H, CH), 5.09 (s, H, CH−Ar), 6.03 (s, 2H, NH), 6.85–8.24 (m, 7H, Ar), 8.43 (d, 2H, CH═CH), 9.83 (s, H, OH). ^{13}C NMR (100 MHz, DMSO-d_6) δ/ppm: 15.3(CH_3), 18.3 (CH_3), 39.2 (C−H, Ar), 60.7(CH_2), 97.9, 105.7, 117.6, 121.5, 124.6, 125.4, 126.2, 127.9, 128.6, 131.3, 134.5 (C−Ar), 145.3 (C−N), 124.3, 150.3 (C═O), 151.8 (C═C), 158.7 (C═O), 168.2 (C═O), 177.7 (C−OH), 182.2 (C═O). MS (*m/z*, (relative abundance, %)): 520 (M^{+1}, 8), 447 (100), 337 (45), 184 (19), 74 (32).

Ethyl 4-(4-hydroxy-3-(3-(4-hydroxy phenyl)acryloyl)-2-oxo-2H-chromen-8-yl)-6-methyl-2-oxo-1,2,3,4-tetrahydropyrimidine-5-carboxylate (DPCU 5): Brown solid; yield 57.92%; m.p. 206–208 °C; IR (KBr, cm^{-1}): v 3368(O−H), 3220(N−H), 2921 (C−H Ar), 2851 (C−H), 1745(C═O), 1674(C═O), 1601, 1474 (C═C), 1283 (C−O), 759 (p-sub); ^{1}H NMR (400 MHz, DMSO-d_6, δ/ppm): 1.62 (t, 3H, CH), 1.98(s, 3H, CH), 4.02(q, 2H, CH), 4.95 (s, H, CH−Ar), 5.58 (s, H, OH), 6.09 (s, 2H, NH), 6.62–7.24 (m, 7H, Ar), 7.94 (d, 2H, CH═CH), 9.44 (s, H, OH). ^{13}C NMR (100 MHz, DMSO-d_6) δ/ppm: 15.6 (CH_3), 17.37 (CH_3), 40.5(C−H, Ar), 61.3 (CH_2), 99.3,106.8, 115.6, 117.2, 125.1, 126.9, 127.2, 128.3, 147.6,148.7 (Ar−C), 150.5 (C═O), 152.2 (C═C), 157.4 (C−OH), 159.2 (C═O), 167.5 (C═O), 178.9 (C−OH), 183.6 (C═O). MS (*m/z*, (relative abundance, %)): 491 (M^{+1}, 9), 398 (28), 308 (100), 184 (53), 94 (19).

Ethyl 4-(4-hydroxy-3- (3-(4-nitrophenyl) acryloyl)-2-oxo-2H-chromen-8-yl)-6-methyl-2-oxo-1,2,3,4-tetrahydropyrimidine-5-carboxylate (DPCU 6). Brown solid; yield 61.39%; m.p. 227–229 °C; IR (KBr, cm^{-1}): v 3471(O−H), 3156(N−H), 2922 (C−H Ar), 2852 (C−H), 1731(C═O), 1667(C═O), 1611, 1474 (C═C), 1550, 1352 (N−O), 1255 (C−O), 758 (p-sub); ^{1}H NMR (400 MHz, DMSO-d_6, δ/ppm): 1.41 (t,3H, CH), 2.04 (s, 3H, CH), 4.12 (q, 2H, CH), 4.93 (s, H CH−Ar), 6.13 (s, 2H, NH), 6.95–8.24 (m, 9H, Ar), 9.38 (s, H, OH). ^{13}C NMR (100 MHz, DMSO-d_6) δ/ppm: 16.2 (CH_3), 20.5 (CH_3), 41.7(C−H, Ar), 62.8 (CH_2), 98.7,106.2, 117.7, 121.6, 124.3, 125.8, 126.3, 127.7, 128.1, 147.5,148.2 (Ar−C), 150.8 (C═C), 152.6 (C−O), 159.7 (C═O), 167.6 (C═O), 178.4 (C═O), 183.4 (C═O). MS (*m/z*, (relative abundance, %)): 520 (M^{+1}, 7), 398 (47), 334 (100), 184 (28), 123 (31).

Ethyl 4-(3-(3-(4-chlorophenyl) acryloyl)-4-hydroxy-2-oxo-2H-chromen-8-yl)-6-methyl-2-oxo-1,2,3,4-tetrahydropyrimidine-5-carboxylate (DPCU 7). Golden yellow solid; yield 67.44%; m.p. 192–194 °C; IR (KBr, cm^{-1}): v 3341(O−H), 3009(N−H), 2924 (C−H Ar), 2852 (C−H), 1737(C═O), 1671(C═O), 1601, 1475 (C═C), 1284 (C−O), 763 (p-sub); ^{1}H NMR (400 MHz, DMSO-d_6, δ/ppm): 1.27 (t, 3H, CH), 1.93 (s, 3H, CH), 4.06 (q, 2H, CH), 4.92 (s, H, CH, Ar), 6.10 (s, 2H, NH), 6.90–7.29 (m, 7H, Ar), 7.79 (d, 2H, CH═CH), 9.31 (s, H, OH). ^{13}C NMR (100 MHz, DMSO-d_6) δ/ppm: 15.5 (CH_3), 18.3 (CH_3), 39.9 (C−, Ar), 60.3 (CH_2), 98.2,106.6, 117.4, 124.2, 125.5, 126.8, 127.5, 128.8, 147.2,148.7 (Ar−C), 150.4 (C═O), 152.2 (C═C), 159.2 (C═O), 167.4 (C═O), 179.8 (C−OH), 183.2 (C═O). MS (*m/z*, (relative abundance, %)): 509 (M^{+1}, 10), 398 (42), 326 (100), 184 (34), 112 (41).

Ethyl-4-(3-(3-(4-(dimethylamino)phenyl)acryloyl)-4-hydroxy-2-oxo-2H-chromen-8-yl)-6-methyl-2-oxo-1,2,3,4-tetrahydropyrimidine-5-carboxylate (DPCU 8). Dark brown solid; yield 72.68%; m.p. 217–219 °C; IR (KBr, cm^{-1}): v 3403(O−H), 3165(N−H), 2923 (C−H Ar), 2854 (C−H), 1727(C═O), 1662(C═O), 1611, 1474 (C═C), 1267 (C−O), 767 (p-sub); ^{1}H NMR (400 MHz, DMSO-d_6, δ/ppm): 1.42 (t, 3H, CH), 2.21 (s, 3H, CH), 2.94 (s, 6H, CH), 4.14 (q, 2H, CH), 5.02 (s, H, CH), 6. 15 (s, 2H, NH), 6.52–7.20 (m, 7H, Ar), 7.75 (d, 2H, CH═CH), 9.26 (s, H, OH). ^{13}C NMR (100 MHz, DMSO-d_6) δ/ppm: 14.8 (CH_3), 19.7 (CH_3), 37.3 (C−H, Ar), 41.3 (N−CH_3), 61.4 (CH_2), 98.7,106.3, 117.8, 124.6, 125.8, 126.3, 127.4, 128.6, 147.6,148.4 (Ar−C), 150.1 (C═O), 152.6 (C═C), 159.8 (C═O), 167.1 (C═O), 179.4 (C−OH), 183.4 (C═O). MS (*m/z*, (relative abundance, %)): 518 (M^{+1}, 8), 398 (56), 335 (100), 174 (26), 121 (39).

Ethyl 4-(4-hydroxy-3-(3-(2-hydroxyphenyl) acryloyl)-2-oxo-2H-chromen-8-yl)-6-methyl-2-oxo-1,2,3,4-tetrahydropyrimidine-5-carboxylate (DPCU 9). Orange solid; yield 54.82%; m.p. 261–263 °C; IR (KBr, cm^{-1}): v 3428(O−H), 3171(N−H), 2925 (C−H Ar), 2850 (C−H), 1733(C═O), 1670(C═O), 1611, 1474 (C═C), 1281 (C−O), 757 (o-sub); ^{1}H NMR (400 MHz, DMSO-d_6, δ/ppm): 1.32 (t, 3H, CH), 2.14 (s, 3H, CH), 4.11 (q, 2H, CH), 4.94 (s, H, CH, Ar), 5.14 (s, H, OH), 6.06 (s,

2H, NH), 6.70–7.20 (m, 7H, Ar), 8.12 (d, 2H, CH═CH), 10.21 (s, H, OH). ^{13}C NMR (100 MHz, DMSO-d_6) δ/ppm: 14.6 (CH_3), 20.5 (CH_3), 40.6 (C−H, Ar), 60.5 (CH_2), 97.2, 106.4, 115.9, 116.5, 117.8, 121.4, 124.4, 125.6, 126.7, 128.1, 147.2, 148.7 (Ar−C), 150.4 (C═O), 152.3 (C═C), 159.2 (C═O), 167.6 (C═O), 178.5 (C−O), 183.7 (C═O). MS (*m/z*, (relative abundance, %)): 491 (M^{+1}, 11), 398 (45), 308 (100), 184 (28), 94 (22).

Ethyl 4-(4-hydroxy-3-(3-(3-hydroxyphenyl) acryloyl)-2-oxo-2H-chromen-8-yl)-6-methyl-2-oxo-1,2,3,4-tetrahydropyrimidine-5-carboxylate (DPCU 10). Yellow solid; yield 60.26%; m.p. 261–263 °C; IR (KBr, cm^{-1}): v 3420(O−H), 3239(N−H), 2924 (C−H Ar), 2853 (C−H), 1733(C═O), 1672(C═O), 1611, 1474 (C═C), 1282 (C−O), 758 (m-sub); ^{1}H NMR (400 MHz, DMSO-d_6, δ/ppm): 1.46 (t, 3H, CH), 2.15 (s, 3H, CH), 4.09 (q, 2H, CH), 5.01 (s, H, OH), 5.21 (s, H, CH, Ar), 6.15 (s, 2H, NH), 6.60–7.19 (m, 7H, Ar), 7.70 (d, 2H, CH═CH), 9.52 (s, H, OH). ^{13}C NMR (100 MHz, DMSO-d_6) δ/ppm: 14.7 (CH_3), 19.2 (CH_3), 38.9 (C−H, Ar), 61.2 (CH_2), 99.7, 106.8, 112.5, 115.3, 117.5, 119.6, 124.6, 125.4, 126.3, 128.8, 147.6, 148.5 (Ar−C), 150.7 (C═O), 152.9 (C═C), 158.3 (C−O), 159.6 (C═O), 167.4 (C═O), 179.4 (C−O), 183.5 (C═O). MS (*m/z*, (relative abundance, %)): 491 (M^{+1}, 9), 418 (30), 326 (100), 215 (43), 94 (25).

Ethyl 4-(4-hydroxy-3-(3-(3-nitrophenyl) acryloyl)-2-oxo-2H-chromen-8-yl)-6-methyl-2-oxo-1,2,3,4-tetrahydropyrimidine-5-carboxylate (DPCU 11). Greenish white solid; yield 55.80%; m.p. 222–224 °C; IR (KBr, cm^{-1}): v 3344(O−H), 3011(N−H), 2926 (C−H Ar), 2853 (C−H), 1736(C═O), 1670(C═O), 1609, 1475 (C═C), 1284 (C−O), 764 (m-sub); ^{1}H NMR (400 MHz, DMSO-d_6, δ/ppm): 1.52 (t, 3H, CH), 2.14 (s, 3H, CH), 4.13 (q, 2H, CH), 5.11 (s, H, CH, Ar), 6.07 (s, 2H, NH), 6.90–8.32 (m, 9H, Ar), 9.57 (s, H, OH). ^{13}C NMR (100 MHz, DMSO-d_6) δ/ppm: 15.5 (CH_3), 20.6 (CH_3), 41.3 (C−H, Ar), 60.7 (CH_2), 99.2, 106.3, 117.7, 120.6, 121.1, 124.4, 125.6, 126.4, 128.5, 129.7, 132.3, 136.8, 147.3, 148.7 (Ar−C), 150.5 (C═O), 152.5 (C═C), 159.3 (C═O), 167.6 (C═O), 179.2 (C−O), 183.7 (C═O). MS (*m/z*, (relative abundance, %)): 520 (M^{+1}, 8), 398 (31), 337 (100), 184 (57), 123 (38).

Ethyl 4-(3-(3-(2-chlorophenyl) acryloyl)-4-hydroxy-2-oxo-2H-chromen-8-yl)-6-methyl-2-oxo-1,2,3,4-tetrahydropyrimidine-5-carboxylate (DPCU 12). Brown solid; yield 61.41%; m.p. 192–194 °C; IR (KBr, cm^{-1}): v 3342(O−H), 3011(N−H), 2926 (C−H Ar), 2854 (C−H), 1738(C═O), 1666(C═O), 1602, 1475 (C═C), 1284 (C−O), 765 (o-sub); ^{1}H NMR (400 MHz, DMSO-d_6, δ/ppm): 1.37 (t, 3H, CH), 1.92 (s, 3H, CH), 4.03 (q, 2H, CH), 5.22 (s, H, CH, Ar), 6.04 (s, 2H, NH), 6.90–7.30 (m, 7H, Ar), 7.98 (d, 2H, CH═CH), 9.62 (s, H, OH). ^{13}C NMR (100 MHz, DMSO-d_6) δ/ppm: 16.3 (CH_3), 21.2 (CH_3), 40.6 (C−H, Ar), 61.5 (CH_2), 99.6, 106.7, 117.2, 124.6, 125.2, 126.8, 127.3, 128.8, 129.3, 131.4, 133.6, 147.5, 148.2 (Ar−C), 150.1 (C═O), 152.8 (C═C), 159.7 (C═O), 167.4 (C═O), 179.5 (C−O), 183.3 (C═O). MS (*m/z*, (relative abundance, %)): 510 (M^{+2}, 10), 398 (47), 326 (100), 184 (26), 112 (17).

Ethyl 4-(4-hydroxy-2-oxo-3-(3-(3,4,5-trimethoxy phenyl)acryloyl)-2H-chromen-8-yl)-6-methyl-2-oxo-1,2,3,4-tetrahydropyrimidine-5-carboxylate (DPCU 13). Brick red solid; yield 73.22%; m.p. 287–289 °C; IR (KBr, cm^{-1}): v 3400(O−H), 3120(N−H), 2936 (C−H Ar), 2850 (C−H), 1734(C═O), 1675(C═O), 1611, 1474 (C═C), 1284 (C−O), 759 (3,4,5-sub); ^{1}H NMR (400 MHz, DMSO-d_6, δ/ppm): 1.27 (t, 3H, CH), 2.03 (s, 3H, CH), 3.79 (s, 9H, CH), 4.31 (s, 2H, CH), 6.05 (s, 2H, NH), 6.20–7.15 (m, 5H, aromatic), 7.84 (d, 2H, CH═CH), 9.52 (s, H, OH). ^{13}C NMR (100 MHz, DMSO-d_6) δ/ppm: 15.6 (CH_3), 19.6 (CH_3), 41.4 (C−H, Ar), 55.3 (O−CH_3), 60.3 (CH_2), 98.3, 103.7, 106.5, 117.6, 124.3, 125.6, 126.5, 138.4, 147.2, 148.6, 149.9 (Ar−C), 150.9 (C═O), 152.7 (C═C), 159.4 (C═O), 167.7 (C═O), 179.2 (C−O), 183.5 (C═O). MS (*m/z*, (relative abundance, %)): 565 (M^{+1}, 7), 398 (59), 382 (38), 216 (100), 184 (23), 168 (15).

Ethyl 4-(3-cinnamoyl-4-hydroxy-2-oxo-2H-chromen-8-yl)-6-methyl-2-thioxo-1,2,3,4-tetrahydropyrimidine-5-carboxylate (DPCT 1). Yellow solid; yield 64.29%; m.p. 127–129 °C; IR (KBr, cm^{-1}): v 3458(O−H), 3128(N−H), 2929 (C−H Ar), 2863(C−H), 1746(C═O), 1602, 1475 (C═C); 1257 (C−O), 765; ^{1}H NMR (400 MHz, DMSO-d_6, δ/ppm): 1.25 (t, 3H, CH), 1.84 (s, 3H, CH), 2.35 (s, 2H, NH), 4.31 (q, 2H, CH), 5.21(s, H, CH−Ar), 6.90–7.38 (m, 8H, Ar), 7.63 (d, 2H, HC═CH), 9.74 (s, H, OH). ^{13}C NMR (100 MHz, DMSO-d_6) δ/ppm: 15.2 (CH_3), 21.5 (CH_3), 45.7 (CH, Ar), 62.4 (CH_2), 98.6, 104.7, 117.4, 124.5, 125.2, 126.5, 128.8, (Ar−C), 152.7 (C═C), 159.2 (C═O), 160.2 (C−N), 167.1 (C═O), 174.8 (C═S), 179.6 (C−O), 183.5 (C═O). MS (*m/z*, (relative abundance, %)): 491 (M^{+1}, 8), 414 (47), 292 (100), 200 (34), 132 (27), 78(19).

Ethyl 4-(4-hydroxy-3-(3-(4-methoxyphenyl) acryloyl)-2-oxo-2H-chromen-8-yl)-6-methyl-2-thioxo-1,2,3,4-tetrahydropyrimidine-5-carboxylate (DPCT 2). Dark red solid; yield 60.47%; m.p. 178–180 °C; IR (KBr, cm^{-1}): v 3379(O−H), 3238(N−H), 2932 (C−H Ar), 2875(C−H), 1730(C═O), 1612, 1474 (C═C); 1281 (C−O), 755(p-sub); ^{1}H NMR (400 MHz, DMSO-d_6, δ/ppm):): 1.31 (t, 3H, CH), 2.16 (s, 3H, CH), 3.67 (s, 3H, CH), 4.28 (q, 2H, CH), 5.07 (s, H, CH−Ar), 6.70–7.20 (m, 9H, Ar), 7.70 (d, 2H, HC═CH), 9.54 (s, H, OH). ^{13}C NMR (100 MHz, DMSO-d_6) δ/ppm: 14.7 (CH_3), 20.4 (CH_3), 45.2 (C−CH), 55.4 (CH_3), 61.6 (CH_2), 99.2, 103.6, 114.4, 117.6, 124.6, 125.7, 126.2, 127.4, 128.7, 148.5, (Ar−C), 152.7 (CH═CH) 159.2 (C═O), 159.9 (C-OCH_3),160.6 (C−N),167.5 (C═O), 179.3 (C−OH), 183.4 (C═O). MS (*m/z*, (relative abundance, %)): 521 (M^{+1}, 11), 414 (62), 322 (23), 200 (14), 108 (35).

Ethyl 4-(4-hydroxy-2-oxo-3-(5-phenylpenta-2, 4-dienoyl)-2H-chromen-8-yl)-6-methyl-2-thioxo-1,2,3,4-tetrahydropyrimidine-5-carboxylate (DPCT 3). Yellow solid; yield 56.72%; m.p. 177–179 °C): IR (KBr, cm^{-1}): v 3379(O−H), 3265(N−H), 2935 (C−H Ar), 2881(C−H), 1732(C═O), 1600, 1474 (C═C); 1281 (C−O), 751; ^{1}H NMR (400 MHz, DMSO-d_6, δ/ppm): 1. 51 (t, 3H, CH), 2.31 (s, 3H, CH), 4.52 (q, 2H, CH), 5.27 (s, H, CH−Ar), 6.85–7.38 (m, 10*H*, Ar), 7.85 (d, 4H, CH═CH), 9.22 (s, H, OH). ^{13}C NMR (100 MHz, DMSO-d_6) δ/ppm: 14.7 (CH_3), 18.2 (CH_3), 45.8 (C−CH), 62.2 (CH_2), 98.2, 104.7, 117.8, 124.2, 125.7, 126.5, 128.1, 128.7, 135.4, 148.1 (Ar−C), 132.4 , 151.2 (CH═CH), 159.1 (C═O), 160.2 (C═O),167.5 (C═O), 174.5 (C═S), 179.6 (C−O), 183.3 (C═O). MS (*m/z*, (relative abundance, %)): 517 (M^{+1}, 10), 440 (61), 318 (52), 200 (47), 78(29).

Ethyl 4-(4-hydroxy-3-(3-(2-nitrophenyl) acryloyl)-2-oxo-2H-chromen-8-yl)-6-methyl-2-thioxo-1,2,3,4-tetrahydropyrimidine-5-carboxylate (DPCT 4). Green solid; yield 69.13%; m.p. 246–248 °C): IR (KBr, cm^{-1}): v 3347(O−H), 3094(N−H), 2930 (C−H Ar), 2867(C−H), 1735(C═O), 1602, 1475 (C═C), 1562, 1355 (N−O), 1257 (C−O), 753(o-sub); ^{1}H NMR (400 MHz, DMSO-d_6, δ/ppm): 1.27 (t, 3H, CH), 2.48 (s, 3H, CH), 4.26 (q, 2H, CH), 5.12 (s, H, CH−Ar), 6.82–8.18 (m, 9H, Ar), 8.31 (d, 2H, CH═CH), 9.62 (s, H, OH). ^{13}C NMR (100 MHz, DMSO-d_6) δ/ppm: 14.7 (CH_3), 19.6 (CH_3), 45.3 (C−H, Ar), 61.4 (CH_2), 98.6, 104.2, 117.1, 121.8, 124.2, 125.6, 126.4, 127.5, 128.1, 130.5, 134.3 (C−Ar), 146.4 (C−N), 155.5 (C═C), 159.2 (C═O), 160.1 (C−N), 167.6 (C═O), 174.2 (C═S), 179.4 (C−O), 183.6 (C═O). MS (*m/z*, (relative abundance, %)): 536 (M^{+1}, 9), 414 (49), 337 (100), 200 (24), 123 (62).

Ethyl 4-(4-hydroxy-3-(3-(4-hydroxyphenyl) acryloyl)-2-oxo-2H-chromen-8-yl)-6-methyl-2-thioxo-1,2,3,4-tetrahydropyrimidine-5-carboxylate (DPCT 5). Brown solid; yield 54.47%; m.p. 208–210 °C; IR (KBr, cm^{-1}): v 3342(O−H), 3217(N−H), 2935 (C−H Ar), 2859(C−H), 1739(C═O), 1610, 1473 (C═C); 1282 (C−O), 754(p-sub); ^{1}H NMR (400 MHz, DMSO-d_6, δ/ppm): 1.27 (t, 3H, CH), 2.26 (s, 3H, CH), 4.16 (q, 2H, CH), 4.82 (s, H, CH−Ar), 5.11 (s, H, OH), 6.55–7.20 (m, 9H, Ar), 7.79 (d, 2H, CH═CH), 9.57 (s, H, OH). ^{13}C NMR (100 MHz, DMSO-d_6) δ/ppm: 14.8 (CH_3), 19.5 (CH_3), 45.3 (C−H, Ar), 61.8 (CH_2), 98.6,104.2, 115.5, 117.5, 124.3, 125.6, 126.3, 127.7, 128.8, 148.3 (Ar−C), 152.5 (C═C), 157.2 (C−OH), 159.5 (C═O), 160.1 (C−N), 167.8 (C═O), 174.2 (C═S), 178.9 (C−OH), 183.2 (C═O). MS (*m/z*, (relative abundance, %)): 507 (M^{+1}, 12), 414 (56), 308 (100), 200 (39), 94 (23).

Ethyl 4-(4-hydroxy-3-(3-(4-nitrophenyl) acryloyl)-2-oxo-2H-chromen-8-yl)-6-methyl-2-thioxo-1,2,3,4-tetrahydropyrimidine-5-carboxylate (DPCT 6). Brown solid; yield 63.42%; m.p. 255–257 °C; IR

(KBr, cm^{-1}): v 3370(O—H), 3281(N—H), 2943(C—H Ar), 2870(C—H), 1735(C=O), 1613, 1474 (C=C); 1572, 1350 (N—O), 1257 (C—O), 751(p-sub); ^{1}H NMR (400 MHz, DMSO-d_6, δ/ppm): 1.39 (t,3H, CH), 2.26 (s, 3H, CH), 4.02 (q, 2H, CH), 5.20 (s, H CH—Ar), 6.87–7.52 (m, 9H, Ar), 8.20 (d, 2H, CH=CH), 9.48 (s, H, OH). ^{13}C NMR (100 MHz, DMSO-d_6) δ/ppm: 15.6 (CH_3), 21.3 (CH_3), 44.7 (C—H, Ar), 60.3 (CH_2), 98.4,104.8, 117.6, 121.1, 124.5, 125.7, 126.5, 127.6, 128.4, 148.5 (Ar—C), 147.5 160.7 (C—N), 152.4 (C=C), 159.9 (C=O), 160.4 (C—N), 167.2 (C=O), 174.3 (C=S), 179.8 (C—OH), 183.8 (C=O). MS (*m/z*, (relative abundance, %)): 536 (M^{+1}, 10), 414 (52), 337 (100), 200 (37), 123 (46).

Ethyl 4-(3-(3-(4-chlorophenyl) acryloyl)-4-hydroxy-2-oxo-2H-chromen-8-yl)-6-methyl-2-thioxo-1,2,3,4-tetrahydropyrimidine-5-carboxylate (DPCT 7). Golden yellow solid; yield 56.75%; m.p. 170–172 °C; IR (KBr, cm^{-1}): v 3394(O—H), 3010(N—H), 2938 (C—H Ar), 2841(C—H), 1738(C=O), 1601, 1474 (C=C); 1286 (C—O), 755 (p-sub); ^{1}H NMR (400 MHz, DMSO-d_6, δ/ppm): 1.06 (t, 3H, CH), 2.39 (s, 3H, CH), 4.37 (q, 2H, CH), 5.41 (s, H, CH, Ar), 6.83–7.37 (m, 9H, Ar), 7.85 (d, 2H, CH=CH), 9.44 (s, H, OH). ^{13}C NMR (100 MHz, DMSO-d_6) δ/ppm: 14.7 (CH_3), 19.6 (CH_3), 44.3 (C—H, Ar), 61.7 (CH_2), 98.6,104.5, 117.9, 124.4, 125.7, 126.3, 127.4, 128.7, 148.1 (Ar—C), 133.7 (C—Cl), 152.7 (C=C), 159.6 (C=O), 160.8 (C—N), 167.8 (C=O), 174.8 (C=S), 179.2 (C—OH), 183.7 (C=O). MS (*m/z*, (relative abundance, %)): 525 (M^{+1}, 6), 414 (33), 326 (100), 200 (58), 112 (27).

Ethyl 4-(3-(3-(4-(dimethylamino) phenyl)acryloyl)-4-hydroxy-2-oxo-2H-chromen-8-yl)-6-methyl-2-thioxo-1,2,3,4-tetra-hydropyrimidine-5-carboxylate (DPCT 8). Dark brown solid; yield 71.37%; m.p. 191–193 °C; IR (KBr, cm^{-1}): v 3400(O—H), 3281(N—H), 3003 (C—H Ar), 2927(C—H), 1739(C=O), 1615, 1475 (C=C); 1281 (C—O), 1167 (C—N), 764 (p-sub); ^{1}H NMR (400 MHz, DMSO-d_6, δ/ppm): 1.22 (t, 3H, CH), 2.21 (s, 3H, CH), 2.88 (s, 6H, CH), 4.21 (q, 2H, CH), 5.17 (s, H, CH), 6.50–7.28 (m, 9H, Ar), 7.88 (d, 2H, CH=CH), 9.51 (s, H, OH). ^{13}C NMR (100 MHz, DMSO-d_6) δ/ppm: 15.6 (CH_3), 20.3 (CH_3), 40.7 (N—CH_3), 45.7 (C—H, Ar), 61.6 (CH_2), 98.2,104.1, 114.6, 117.2, 124.6, 125.4, 126.5, 127.8, 128.3, (Ar—C), 148.4, 160.4 (C—N), 152.3 (C=C), 159.8 (C=C), 167.5 (C=O), 174.3 (C=S), 179.1 (C—OH), 183.8 (C=O). MS (*m/z*, (relative abundance, %)): 534 (M^{+1}, 11), 414 (54), 335 (100), 200 (19), 121 (61).

Ethyl 4-(4-hydroxy-3-(3-(2-hydroxyphenyl) acryloyl)-2-oxo-2H-chromen-8-yl)-6-methyl-2-thioxo-1,2,3,4-tetrahydropyrimidine-5-carboxylate (DPCT 9). Orange solid; yield 58.56%; m.p. 208–210 °C; IR (KBr, cm^{-1}): v 3426(O—H), 3104(N—H), 2934 (C—H Ar), 2867(C—H), 1737(C=O), 1611, 1474 (C=C); 1287 (C—O), 751(o-sub);^{1}H NMR (400 MHz, DMSO-d_6, δ/ppm): 1.24 (t, 3H, CH), 2.18 (s, 3H, CH), 4.22 (q, 2H, CH), 5.08 (s, H, CH, Ar), 5.52 (s, H, OH), 6.55–7.31 (m, 9H, Ar), 8.02 (d, 2H, CH=CH), 10.13 (s, H, OH). ^{13}C NMR (100 MHz, DMSO-d_6) δ/ppm: 16.3 (CH_3), 20.9 (CH_3), 45.2 (C—H, Ar), 61.3 (CH_2), 98.3, 104.7, 115.3, 116.9, 117.7, 121.8, 124.2, 125.1, 126.9, 128.8, 148.2 (Ar—C), 152.7 (C=C), 159.7 (C=O), 167.4 (C=O), 178.8 (C—O), 183.1 (C=O). MS (*m/z*, (relative abundance, %)): 507 (M^{+1}, 7), 414 (59), 308 (100), 200 (20), 94 (35).

Ethyl 4-(4-hydroxy-3-(3-(3-hydroxyphenyl) acryloyl)-2-oxo-2H-chromen-8-yl)-6-methyl-2-thioxo-1,2,3,4-tetrahydropyrimidine-5-carboxylate (DPCT 10). Yellow solid; yield 62.37%; m.p. 206–208 °C; IR (KBr, cm^{-1}): v 3346(O—H), 3219(N—H), 2939 (C—H Ar), 2885(C—H), 1731(C=O), 1611, 1474 (C=C); 1251 (C—O), 757(o-sub); ^{1}H NMR (400 MHz, DMSO-d_6, δ/ppm): 1.28 (t, 3H, CH), 2.20 (s, 3H, CH), 4.27 (q, 2H, CH), 4.69 (s, H, OH), 5.37 (s, H, CH, Ar), 6.51–7.10 (m, 9H, Ar), 7.86 (d, 2H, CH=CH), 9.69 (s, H, OH). ^{13}C NMR (100 MHz, DMSO-d_6) δ/ppm: 16.5 (CH_3), 20.6 (CH_3), 44.8 (C—H, Ar), 60.7 (CH_2), 98.1, 104.2, 112.9, 115.8, 117.1, 119.2, 124.2, 125.8, 126.9, 128.2, 148.8 (Ar—C), 152.3 (C=C), 158.2 (C—O), 159.8 (C=O), 160.7 (C—N), 167.8 (C=O), 174.8 (C=S), 179.1 (C—O), 183.7 (C=O). MS (*m/z*, (relative abundance, %)): 507 (M^{+1}, 6), 414 (63), 308 (100), 200 (26), 94 (44).

Ethyl 4-(4-hydroxy-3-(3-(3-nitrophenyl) acryloyl)-2-oxo-2H-chromen-8-yl)-6-methyl-2-thioxo-1,2,3,4-tetrahydropyrimidine-5-carboxylate (DPCT 11). Greenish white solid; yield 59.45%; m.p. 236–238 °C; IR (KBr, cm^{-1}): v 3458(O—H), 3128(N—H), 2929 (C—H Ar), 2863(C—H), 1746(C=O), 1602, 1475 (C=C); 1568, 1347 (N—O), 1257 (C—O), 765 (m-sub); ^{1}H NMR (400 MHz, DMSO-d_6, δ/ppm): 1.31 (t, 3H, CH), 2.30 (s, 3H, CH), 4.22 (q, 2H, CH), 5.25 (s, H, CH, Ar), 6.79–7.68 (m, 9H, Ar), 8.30 (d, 2H, CH=CH), 9.45 (s, H, OH). ^{13}C NMR (100 MHz, DMSO-d_6) δ/ppm: 14.9 (CH_3), 19.6 (CH_3), 45.2 (C—H, Ar), 60.9 (CH_2), 98.7, 104.8, 117.6, 120.3, 121.7, 124.8, 125.2, 126.2, 128.8, 129.4, 132.7, 136.6, (Ar—C), 148.7 (C-NO_2), 152.9 (C=C), 159.1 (C=O), 160.8 (C—N), 167.5 (C=O), 174.7 (C=S), 179.1 (C—O), 183.7 (C=O). MS (*m/z*, (relative abundance, %)): 536 (M^{+1}, 12), 414 (55), 337 (100), 184 (67), 123 (28).

Ethyl 4-(3-(3-(2-chlorophenyl) acryloyl)-4-hydroxy-2-oxo-2H-chromen-8-yl)-6-methyl-2-thioxo-1,2,3,4-tetrahydropyrimidine-5-carboxylate (DPCT 12). Brown crystals; yield 58.72%; m.p. 171–173 °C; IR (KBr, cm^{-1}): v 3369(O—H), 3249(N—H), 2939(C—H Ar), 2865(C—H), 1732(C=O), 1600, 1474 (C=C); 1281 (C—O), 765(o-sub); ^{1}H NMR (400 MHz, DMSO-d_6, δ/ppm): 1.42 (t, 3H, CH), 2.27 (s, 3H, CH), 4.33 (q, 2H, CH), 5.03 (s, H, CH, Ar), 6.88–7.39 (m, 9H, Ar), 7.63 (d, 2H, CH=CH), 9.41 (s, H, OH). ^{13}C NMR (100 MHz, DMSO-d_6) δ/ppm: 15.8 (CH_3), 19.4 (CH_3), 45.2 (C—H, Ar), 61.9 (CH_2), 98.3, 104.8, 117.2, 124.1, 125.4, 126.7, 127.1, 128.8, 129.7, 131.2, 133.9, 148.5 (Ar—C), 152.3 (C=C), 159.3 (C=O), 160.7 (C—N), 167.8 (C=O), 174.7 (C=S), 179.8 (C—O), 183.7 (C=O). MS (*m/z*, (relative abundance, %)): 526 (M^{+2}, 13), 414 (38), 326 (100), 200 (69), 112 (48).

Ethyl 4-(4-hydroxy-2-oxo-3-(3-(3,4,5-trimethoxyphenyl)acryloyl)-2H-chromen-8-yl)-6-methyl-2-thioxo-1,2,3,4-tetra-hydropyrimidine-5-carboxylate (DPCT 13). Brick red solid; yield 70.33%; m.p. 263–265 °C; IR (KBr, cm^{-1}): v 3356(O—H), 3216(N—H), 2939 (C—H Ar), 2839(C—H), 1735(C=O), 1610, 1474 (C=C); 1281 (C—O), 755 (3,4,5-sub); ^{1}H NMR (400 MHz, DMSO-d_6, δ/ppm): 1.36 (t, 3H, CH), 2.32 (s, 3H, CH),3.88 (s, 9H, CH), 4.34 (q, 2H, CH), 4.91 (s, H, CH), 6.15–7.10 (m, 7H, Ar), 7.68 (d, 2H, CH=CH), 9.72 (s, H, OH). ^{13}C NMR (100 MHz, DMSO-d_6) δ/ppm: 16.4 (CH_3), 20.3 (CH_3), 44.8 (C—H, Ar), 56.9 (O—CH_3), 61.6 (CH_2), 98.7, 103.1, 104.3, 106.5, 117.2, 124.5, 125.8, 126.2, 128.2, 138.1, 148.6, 149.9 (Ar—C), 150.5 (C-OCH_3), 152.3 (C=C), 159.9 (C=O), 160.3 (C—N), 167.5 (C=O), 174.9 (C=S), 179.7 (C—O), 183.1 (C=O). MS (*m/z*, (relative abundance, %)): 581 (M + 1, 9), 414 (48), 382 (100), 200 (23), 168 (15).

5-cinnamoyl-4-(4-hydroxy-2-oxo-2H-chromen-8-yl)-6-methyl-3,4,dihydropyrimidin2(1H)-one (DCCU 1). The was found to be Yellow solid; yield 65.41%; m.p. 153–155 °C; IR (KBr, cm^{-1}): v 3479(N—H), 3370(O—H), 3060 (C—H Ar), 2925(C—H), 1734(C=O), 1671(C=O), 1601, 1471 (C=C), 1282, 1056 (C—O—C); ^{1}H NMR (400 MHz, DMSO-d_6, δ/ppm): 2.50(s, 3H, CH), 4.95(s, H, CH), 6.9 (s, 2H, NH) 7.42–7.65 (m, 9H, aromatic), 8.32 (d, 2H, HC=CH), 9.11(s, H, OH). ^{13}C NMR (100 MHz, DMSO-d_6) δ/ppm: 17.7 (CH_3), 42.5(C—CH), 117.4, 121.3, 125.2, 126.5, 127.9, 128.4, 128.5, 128.6, 135.2, 148.3, 154.8 (Ar—C), 193.3 (C=O), 150.2 (C=O), 162.2 (C=O), 166.1(C—O), 142.2 (C=C). MS (*m/z*, (relative abundance, %)): 403 (M^{+1}, 25.6), 271 (47), 243 (100), 162 (54), 132 (36).

4-(4-hydroxy-2-oxo-2H-chromen-8-yl)-5-(3-(4-methoxyphenyl) acryloyl)-6-methyl-3,4-dihydropyrimidin2(1H)-one (DCCU 2). Dark red solid; yield 62.76%; m.p. 168–170 °C; IR (KBr, cm^{-1}): v 3436(N—H), 3362(O—H), 2928 (C—H Ar), 2840(C—H), 1732(C=O), 1665(C=O), 1611, 1474 (C=C), 1252, 1054 (C—O—C), 830 (o-sub); ^{1}H NMR (400 MHz, DMSO-d_6, δ/ppm): 2.54(s, 3H, CH), 3.78 (s, 3H, CH), 4.91(s, H, CH), 6.9 (s, 2H, NH), 7.34–7.84 (m, 8H, aromatic), 8.37 (d, 2H, HC=CH), 9.11(s, H, OH). ^{13}C NMR (100 MHz, DMSO-d_6) δ/ppm: 17.9 (CH_3), 42.2(C—CH), 54.3(CH), 91.4, 114.4, 117.6, 118.2, 121.1, 123.7, 125.6, 126.1, 127.3, 128.7, 130.4, 154.3, 159.2 (Ar—C), 193.5 (C=O), 150.4 (C=O), 162.6 (C=O), 166.5(C—O), 142.6 (C=C). MS (*m/z*, (relative abundance, %): 433 (M^{+1}, 26.4), 327 (100), 272 (36), 162 (28), 108 (57).

4-(4-hydroxy-2-oxo-2H-chromen-8-yl)-6-methyl-5-(5-

phenylpenta-2,4-dienoyl)-3,4-dihydropyrimidin2(1H)-one (DCCU 3). Yellow solid; yield 72.28%; m.p. 151–152 °C; IR (KBr, cm^{-1}): v 3462(N−H), 3269(O−H), 3038 (C−H Ar), 2923(C−H), 1739(C=O), 1674(C=O), 1601, 1474 (C=C), 1258, 1057 (C−O−C); ^{1}H NMR (400 MHz, DMSO-d_6, δ/ppm): 2.48(s, 3H, CH), 4.74 (s, H, CH), 6.12 (s, 2H, NH), 6.6–7.41 (m, 9H, aromatic), 7.82 (dd, 4H, C=C), 9.05 (s, H, OH). ^{13}C NMR (100 MHz, DMSO-d_6) δ/ppm: 17.6 (CH_3), 42.1(C−CH), 91.2, 117.3, 118.5, 121.5, 125.4, 126.3, 127.2, 128.3, 128.6, 135.4, 154.2 (Ar−C), 193.2 (C=O), 150.1 (C=O), 162.4 (C=O), 166.6 (C−O), 141.3 (C=C), 151.4 (C=C). MS (*m/z*, (relative abundance, %)): 429 (M^{+1}, 27.5), 327 (100), 272 (36), 162 (28), 108 (57).

4-(4-hydroxy-2-oxo-2H-chromen-8-yl)-6-methyl-5-(3-(2-nitrophenyl)acryloyl)-3,4-dihydropyrimidin2(1H)-one (DCCU 4). Green solid; yield 57.37%; m.p. 117–1119 °C; IR (KBr, cm^{-1}): v 3445(N−H), 3378(O−H), 3042(C−H Ar), 2925(C−H), 1672(C=O), 1608 (C=C), 1531,1384 (Nitro), 1236 (C−O−C) 756 (o-sub); ^{1}H NMR (400 MHz, DMSO-d_6, δ/ppm): 2.49(s, 3H, CH), 4.93 (s, H, CH), 7.10 (s, 2H, NH) 7.36–8.10 (m, 8H, aromatic), 8.45 (d, 2H, HC=CH), 9.09 (s, H, OH). ^{13}C NMR (100 MHz, DMSO-d_6) δ/ppm: 18.3 (CH_3), 42.7 (C−CH), 91.2, 117.5, 118.2, 121.1, 123.2, 123.6, 125.1, 126.8, 128.1, 128.4, 134.2, 154.1 (Ar−C), 193.5 (C=O), 150.5 (C=O), 162.8 (C=O), 166.3 (C−O), 147.3 (C−N), 152.6 (C=C). MS (*m/z*, (relative abundance, %)): 448 (M^{+1}, 25.3), 325 (100), 272 (36), 162 (28), 108 (57).

4-(4-hydroxy-2-oxo-2H-chromen-8-yl)-5-(3-(4-hydroxyphenyl) acryloyl)-6-methyl-3,4-dihydropyrimidin2(1H)-one (DCCU 5). Brown solid; yield 66.18%; m.p. 127–129 °C; IR (KBr, cm^{-1}): v 3469(N−H), 3274(O−H), 3056(C−H Ar), 2936(C−H), 1729(C=O), 1670(C=O), 1611, 1474 (C=C), 1255, 1053 (C−O−C), 758 (p-sub); ^{1}H NMR (400 MHz, DMSO-d_6, δ/ppm): 2.27(s, 3H, CH), 4.88(s, H, CH), 5.22 (s, H, OH), 6.78 (s, 2H, NH), 7.15–7.65 (m, 8H, aromatic), 8.17 (d, 2H, HC=CH), 9.56 (s, H, OH). ^{13}C NMR (100 MHz, DMSO-d_6) δ/ppm: 17.95 (CH_3), 43.3(C−CH), 115.2, 117.6, 118.7, 121.7, 123.5, 125.5, 126.3, 127.4, 128.7, 130.4, 154.3 (Ar−C), 193.5 (C=O), 150.1 (C=O), 162.2 (C=O), 166.7 (C−O), 142.6 (C=C), 157.2 (C=O). MS (*m/z*, (relative abundance, %)): 419 (M^{+1}, 27.3), 326 (37), 272 (100), 147 (41), 106 (23).

4-(4-hydroxy-2-oxo-2H-chromen-8-yl)-6-methyl-5-(3-(4-nitrophenyl)acryloyl)-3,4-dihydropyrimidin2(1H)-one (DCCU 6). Brown solid; yield 54.29%; m.p. 173–174 °C; IR (KBr, cm^{-1}): v 3479(N−H), 3113(O−H), 3081(C−H Ar), 2927(C−H), 1763(C=O), 1692(C=O), 1602, 1474 (C=C), 1522,1345 (Nitro), 1282, 1058 (C−O−C), 758 (p-sub); ^{1}H NMR (400 MHz, DMSO-d_6, δ/ppm): 2.42(s, 3H, CH), 4.75(s, H, CH), 7.05(s, 2H, NH), 7.34–7.78 (m, 8H, aromatic), 8.30 (d, 2H, HC=CH), 9.05 (s, H, OH). ^{13}C NMR (100 MHz, DMSO-d_6) δ/ppm: 20.13 (CH_3), 45.6(C−CH), 95.2, 117.9, 118.1, 121.9, 123.5, 124.3, 125.7, 126.8, 128.6, 129.2, 130.1, 141.5, 148.5, 154.2 (Ar−C), 193.6 (C=O), 150.5 (C=O), 162.4 (C=O), 166.4 (C−O), 142.3 (C=C). MS (*m/z*, (relative abundance, %)): 448 (M^{+1}, 27.3), 326 (28), 272 (100), 177 (19), 123 (31).

5-(3-(4-chlorophenyl)acryloyl)-4-(4-hydroxy-2-oxo-2H-chromen-8-yl)-6-methyl-3,4-dihydropyrimidin2(1H)-one (DCCU 7). Golden yellow solid; yield 78.72%; m.p. 182–184 °C; IR (KBr, cm^{-1}): v 3438(N−H), 3238(O−H), 3062(C−H Ar), 2928(C−H), 1732(C=O), 1672(C=O), 1601, 1474 (C=C), 1281, 1057 (C−O−C), 1133 (C−Cl), 758 (p-sub); ^{1}H NMR (400 MHz, DMSO-d_6, δ/ppm): 2.49 (s, 3H, CH), 4.92 (s, H, CH), 7.03–7.75 (m, 12H, aromatic), 9.09 (s, H, OH). ^{13}C NMR (100 MHz, DMSO-d_6) δ/ppm: 20.4 (CH_3), 43.2 (C−CH), 92.1, 117.2, 118.7, 121.5, 123.1, 125.5, 126.2, 128.3, 129.2, 129.9, 133.5, 133.9, 148.5, 154.4 (Ar−C), 193.3 (C=O), 150.1 (C=O), 162.8 (C=O), 166.7 (C−O), 143.5 (C=C). MS (*m/z*, (relative abundance, %)): 438 (M^{+2}, 32.1), 326 (37), 272 (100), 162 (26), 111 (41).

5-(3-(4-(dimethylamino)phenyl)acryloyl)-4-(4-hydroxy-2-oxo-2H-chromen-8-yl)-6-methyl-3,4-dihydropyrimidin2(1H)-one (DCCU 8). Dark brown solid; yield 58.38%; m.p. 144–146 °C; IR (KBr, cm^{-1}): v 3402(N−H), 3225 (O−H), 3032(C−H Ar), 2925(C−H), 1713(C=O), 1608, 1472 (C=C), 1268, 1058 (C−O−C), 765(p-sub); ^{1}H NMR (400 MHz, DMSO-d_6, δ/ppm): 2.47 (s, 3H, CH), 3.10 (s, 6H, CH), 5.05 (s, H, CH), 6.50(s, 2H, NH), 7.25–7.73 (m, 8H, aromatic), 7.95(d, 2H, HC=CH), 9.05 (s, H, OH). ^{13}C NMR (100 MHz, DMSO-d_6) δ/ppm: 20.7 (CH_3), 40. 2 (*N*−CH), 45.1 (C−CH), 92.5, 117.6, 118.2, 121.7, 123.4, 124.4, 125.1, 126.5, 128.7, 129.1, 148.2 (Ar−C), 150.6, 154.4 (Ar−C−N), 193.6 (C=O), 150.4 (C=O), 162.2 (C=O), 166.3 (C−O), 142.1 (C=C). MS (*m/z*, (relative abundance, %)): 446 (M^{+1}, 27.5), 326 (28), 272 (100), 174 (15), 120 (32).

4-(4-hydroxy-2-oxo-2H-chromen-8-yl)-5-(3-(2-hydroxyphenyl) acryloyl)-6-methyl-3,4-dihydropyrimidin2(1H)-one (DCCU 9). Orange solid; yield 68.83%; m.p. 155–157 °C; IR (KBr, cm^{-1}): v 3452(N−H), 3234(O−H), 3062(C−H Ar), 2928(C−H), 1667(C=O), 1601, 1475 (C=C), 1246, 1056 (C−O−C), 757(o-sub); ^{1}H NMR (400 MHz, DMSO-d_6, δ/ppm): 2.38 (s, 3H, CH), 4.74 (s, H, CH), 5.27 (s, H, OH), 6.72(s, 2H, NH), 7.20–7.84 (m, 8H, aromatic), 8.21(d, 2H, HC=CH), 9.51 (s, H, OH). ^{13}C NMR (100 MHz, DMSO-d_6) δ/ppm: 20.2 (CH_3), 43.4 (C−CH), 91.3, 117.4, 118.6, 121.2, 122.2, 123.1, 125.6, 126.3, 128.2, 129.1, 129.5, 148.4 (Ar−C), 154.6 (Ar−C−N), 193.1 (C=O), 150.7 (C=O), 162.8 (C=O), 157.4, 166.7 (C−O), 152.4 (C=C). MS (*m/z*, (relative abundance, %)): 419 (M^{+1}, 25.3), 326 (17), 272 (100), 162 (35), 94 (26).

4-(4-hydroxy-2-oxo-2H-chromen-8-yl)-5-(3-(3-hydroxyphenyl) acryloyl)-6-methyl-3,4-dihydropyrimidin2(1H)-one (DCCU 10). Yellow solid; yield 53.11%; m.p. 136–138 °C; IR (KBr, cm^{-1}): v 3458(N−H), 3237(O−H), 3046(C−H Ar), 2930(C−H), 1730(C=O), 1672(C=O), 1601, 1474 (C=C), 1256, 1058 (C−O−C), 757(m-sub); ^{1}H NMR (400 MHz, DMSO-d_6, δ/ppm): 2.44 (s, 3H, CH), 5.03 (s, H, CH), 5.37 (s, H, OH), 6.78(s, 2H, NH), 7.15–7.77 (m, 8H, aromatic), 8.05 (d, 2H, HC=CH), 9.08 (s, H, OH). ^{13}C NMR (100 MHz, DMSO-d_6) δ/ppm: 20.4 (CH_3), 45.2 (C−CH), 91.2, 115.3, 117.6, 117.8, 118.4, 121.2, 123.5, 125.1, 126.9, 128.4, 130.4, 148.2 (Ar−C), 154.3 (Ar−C−N), 193.4 (C=O), 150.2 (C=O), 162.3 (C=O), 158.2, 166.3 (C−O), 142.5 (C=C). MS (*m/z*, (relative abundance, %)): 419 (M^{+1}, 25.3), 326 (17), 272 (100), 162 (35), 94 (26).

4-(4-hydroxy-2-oxo-2H-chromen-8-yl)-6-methyl-5-(3-(3-nitrophenyl)acryloyl)-3,4-dihydropyrimidin2(1H)-one (DCCU 11). Greenish white solid; yield 59.73%; m.p. 103–105 °C; IR (KBr, cm^{-1}): v 3385(N−H), 3238(O−H), 3049(C−H Ar), 2926(C−H), 1673(C=O), 1609, 1474 (C=C), 1489, 1282 (nitro), 1235, 1050(C−O−C), 753(m-sub); ^{1}H NMR (400 MHz, DMSO-d_6, δ/ppm): 2.38 (s, 3H, CH), 4.89 (s, H, CH), 6.49(s, 2H, NH), 7.13–7.85 (m, 8H, aromatic), 8.52 (d, 2H, HC=CH), 9.81 (s, H, OH). ^{13}C NMR (100 MHz, DMSO-d_6) δ/ppm: 17.8 (CH_3), 41.9 (C−CH), 92.4, 117.9, 118.1, 121.5, 123.8, 125.6, 126.9, 128.1, 130.1, 136.2, 137.9, 148.5 (Ar−C), 147.5, 154.3 (Ar−C−N), 193.2 (C=O), 150.6 (C=O), 162.1 (C=O), 166.7 (C−O), 142.7 (C=C). MS (*m/z*, (relative abundance, %)): 448 (M^{+1}, 25.3), 326 (25), 272 (100), 177 (42), 123 (15).

5-(3-(2-chlorophenyl)acryloyl)-4-(4-hydroxy-2-oxo-2H-chromen-8-yl)-6-methyl-3,4-dihydropyrimidin2(1H)-one (DCCU 12). Brown solid; yield 57.25%; m.p. 106–107 °C; IR (KBr, cm^{-1}): v 3379(N−H), 3167(O−H), 3058(C−H Ar), 2926(C−H), 1673(C=O), 1610, 1476 (C=C), 1235, 1071 (C−O−C), 1129 (C−Cl), 757(o-sub); ^{1}H NMR (400 MHz, DMSO-d_6, δ/ppm): 2.41 (s, 3H, CH), 4.95 (s, H, CH), 6.81 (s, 2H, NH), 6.81–7.45 (m, 8H, aromatic), 8.20 (d, 2H, HC=CH), 9.03 (s, H, OH). ^{13}C NMR (100 MHz, DMSO-d_6) δ/ppm: 20.2 (CH_3), 42.3 (C−CH), 91.7, 117.7, 118.8, 121.3, 123.2, 125.2, 126.4, 127.3, 128.9, 129.1, 130.2, 133.2, 134.4, 148.1 (Ar−C), 154.3 (Ar−C−N), 193.2 (C=O), 150.2 (C=O), 162.6 (C=O), 166.3 (C−O), 122.2 (C=C), 134.5 (C−Cl). MS (*m/z*, (relative abundance, %)): 438 (M^{+2}, 32.5), 326 (31), 272 (100), 166 (38), 112 (44).

4-(4-hydroxy-2-oxo-2H-chromen-8-yl)-6-methyl-5-(3-(3,4,5-trimethoxyphenyl) acryloyl)-3,4-dihydropyrimidin2(1H)-one (DCCU 13). Brick red solid; yield 65.41%; m.p. 153–155 °C; IR (KBr, cm^{-1}): v 3414(N−H), 3234(O−H), 2939(C−H Ar), 2839(C−H), 1675(C=O), 1601 (C=C), 1281, 1055 (C−O−C) 758, 645 (3,4,5-sub); ^{1}H NMR (400 MHz, DMSO-d_6, δ/ppm): 2.47 (s, 3H, CH), 3.91 (s, 9H, CH), 4.78

Table 1
RMSD Values for re-docked co-crystal ligand conformers.

S. No.	Conformer ID	Docking Score	RMSD Value (A^0)
1	Reference Ligand	−68.649	–
2	ANP_C37_LP2.mds	−58.194	3.979
3	ANP_C120_LP4.mds	−60.002	4.984
4	ANP_C29_LP5.mds	−63.006	4.994
5	ANP_C29_P30.mds	−68.848	4.994
6	ANP_C113_LP3.mds	−65.714	4.996
7	ANP_C19_LP4.mds	−68.148	5.011
8	ANP_C19_P29.mds	−68.148	5.011
9	ANP_C20_LP3.mds	−65.333	5.020
10	ANP_C20_LP1.mds	−65.422	5.021
11	ANP_C9_LP3.mds	−62.601	5.022

(s, H, CH), 6.75(s, 2H, NH), 7.22–7.68 (m, 6H, aromatic), 8.10(s, 2H, HC═CH), 9.08 (s, H, OH). ^{13}C NMR (100 MHz, DMSO-d_6) δ/ppm: 20.5 (CH_3), 40.4 (C−CH), 56.5, 60.7 (O−CH_3), 92.4, 103.1, 117.3, 118.5, 121.6, 123.5, 125.7, 126.3, 128.7, 148.5 (Ar−C), 154.5 (Ar−C−N), 193.6 (C═O), 150.7 (C═O), 162.4 (C═O), 138.5, 153.1, 166.3 (C−O), 142.5 (C═C). MS (*m/z*, (relative abundance, %)): 493 (M^{+1}, 28.7), 326 (45), 272 (100), 223 (27), 168 (32).

8-(5-cinnamoyl-6-methyl-2-thioxo-1,2,3,4-tetrahydropyrimidin4-yl)-4-hydroxy-2H-chromen-2-one (DCCT 1). The was found to be Yellow solid; yield 69.46%; m.p. 106–108 °C; IR (KBr, cm^{-1}): v 3472(O−H), 3347(N−H), 2919 (C−H Ar), 2850(C−H), 1671(C═O), 1608,1490 (C═C), 1232, 1039 (C−O); ^{1}H NMR (400 MHz, DMSO-d_6, δ/ppm): 2.42 (s, 3H, CH), 4.85(s, H, CH), 6.35 (s, 2H, NH), 6.37–7.33 (m, 9H, Ar), 7.89 (d, 2H, C═C), 9.12 (s, H, OH). ^{13}C NMR (100 MHz, DMSO-d_6) δ/ppm: 17.2 (CH_3), 43.7 (C−CH), 91.5, 116.7, 117.7, 124.2, 125.8, 126.2, 128.5, 135.3, 148.5, (Ar−C), 160.6 (C═O), 166.1 (C−OH), 167.8(C−N), 174.4 (C═S), 193.8 (C═O). MS (*m/z*, (relative abundance, %)): 419 (M^{+1}, 11), 342 (32), 287 (100), 162 (49), 128 (66), 78(17), 55(24).

4-hydroxy-8-(5-(3-(4-methoxyphenyl)acryloyl)-6-methyl-2-thioxo-1,2,3,4-tetrahydro pyrimidin4-yl)-2H-chromen-2-one (DCCT 2). Dark red solid; yield 61.31%; m.p. 146–148 °C; IR (KBr, cm^{-1}): v 3424(O−H), 3318(N−H), 3055 (C−H Ar), 2948(C−H), 1682(C═O), 1602 (C═C), 1425 (C═C)1287, 1050 (C−O), 759 (o-sub); ^{1}H NMR (400 MHz, DMSO-d_6, δ/ppm): 2.38 (s, 3H, CH), 3.14 (s, 3H, CH), 4.66(s, H, CH), 6.11 (2H, NH), 6.69–7.21 (m, 8H, Ar), 7.61 (d, 2H, C═C), 9.58 (s, H, OH). ^{13}C NMR (100 MHz, DMSO-d_6) δ/ppm: 15.8 (CH_3), 42.9 (C−CH), 55.4 (CH_3), 91.2, 114.5, 116.4, 117.2, 124.6, 125.3, 126.7, 127.8, 128.2, 148.5 (Ar−C), 152.5 (C═C), 158.2 (C-OCH_3), 160.7 (C═O), 166.8 (C−OH), 167.4 (C−N), 174.1 (C═S), 193.2 (C═O), MS (*m/z*, (relative abundance, %)): 449 (M^{+1}, 10), 342 (100), 182 (47), 162 (19), 108 (32).

4-hydroxy-8-(6-methyl-5-(5-phenylpenta-2,4-dienoyl)-2-thioxo-1,2,3,4-tetrahydro pyrimidin4-yl)-2H-chromen-2-one (DCCT 3). Yellow solid; yield 58.52%; m.p. 142–144 °C; IR (KBr, cm^{-1}):v 3415(O−H), 3218(N−H), 3013 (C−H Ar), 2893(C−H), 1688(C═O), 1411 (C═C), 753(Ar); ^{1}H NMR (400 MHz, DMSO-d_6, δ/ppm): 2.56 (s, 3H, CH), 4.85 (s, H, CH), 6.15 (s, 2H, NH), 6.91–7.35 (m, 9H, Ar), 6.68, 7.55 (d, 4H, C═C), 9.47 (s, H, OH). ^{13}C NMR (100 MHz, DMSO-d_6) δ/ppm: 17.3 (CH_3), 43.7(C−CH), 91.8, 116.3, 117.8, 124.6, 125.7, 126.9, 128.4, 135.4 (Ar−C), 131.5, 151.5 (C═C), 160.3 (C═O), 166.2 (C−O), 167.9 (C−N), 174.7 (C═S), 193.4 (C═O). MS (*m/z*, (relative abundance, %)): 445 (M^{+1}, 8), 288 (100), 162 (43), 128 (53), 108 (18).

4-hydroxy-8-(6-methyl-5-(3-(2-nitrophenyl)acryloyl)-2-thioxo-1,2,3,4-tetrahydro pyrimidin4-yl)-2H-chromen-2-one (DCCT 4). Green solid; yield 66.71%; m.p. 152–154 °C; IR (KBr, cm^{-1}): v 3462 (O−H), 3284 (N−H), 3019(C−H Ar), 2938(C−H), 1684(C═O), 1535,1382 (Nitro), 1445(C═C), 1282, 1045(C−O), 783 (p-sub); ^{1}H NMR (400 MHz, DMSO-d_6, δ/ppm): 2.29 (s, 3H, CH), 4.85 (s, H, CH), 6.06 (s, 2H, NH), 6.80–7.38 (m, 8H, Ar), 7.64(d. 2H, C═C), 9.47 (s, H, OH). ^{13}C NMR (100 MHz, DMSO-d_6) δ/ppm: 15.7 (CH_3), 43.8 (C−CH),

Table 2
Docking Scores of Coumarin-Chlacone Hybrids against Insulin protein.

S. No.	Hybrid	Insulin Receptor (1IR3)	S. No	Hybrid	Insulin Receptor (1IR3)
1	DPCU 1	−64.42	29	DCCU 1	−68.23
2	DPCU 2	−63.02	30	DCCU 2	−54.18
3	DPCU 3	−58.64	31	DCCU 3	−53.91
4	DPCU 4	−62.53	32	DCCU 4	−57.77
5	DPCU 5	−61.39	33	DCCU 5	−55.99
6	DPCU 6	**−78.86**	34	DCCU 6	−59.99
7	DPCU 7	−55.35	35	DCCU 7	−53.45
8	DPCU 8	−59.30	36	DCCU 8	**−82.26**
9	DPCU 9	−63.87	37	DCCU 9	−61.05
10	DPCU 10	−64.03	38	DCCU 10	−50.10
11	DPCU 11	−69.35	39	DCCU 11	**−81.30**
12	DPCU 12	−63.22	40	DCCU 12	−50.62
13	DPCU 13	−58.56	41	DCCU 13	**−83.15**
14	DPCT 1	−60.37	42	DCCT 1	−61.62
15	DPCT 2	−61.28	43	DCCT 2	−47.24
16	DPCT 3	−67.19	44	DCCT 3	−68.87
17	DPCT 4	−57.07	45	DCCT 4	−57.77
18	DPCT 5	−59.18	46	DCCT 5	−55.99
19	DPCT 6	−56.68	47	DCCT 6	−59.99
20	DPCT 7	−59.17	48	DCCT 7	−53.45
21	DPCT 8	−71.64	49	DCCT 8	**−81.82**
22	DPCT 9	−63.99	50	DCCT 9	−61.05
23	DPCT 10	−63.09	51	DCCT 10	−50.10
24	DPCT 11	**−79.51**	52	DCCT 11	**−81.30**
25	DPCT 12	−61.44	53	DCCT 12	−50.62
26	DPCT 13	−63.53	54	DCCT 13	**−82.72**
27	Internal ligand (ANP)	−68.64	56	Metformin	−25.15

91.6, 116.2, 117.8, 121.5, 124.2, 125.6, 126.2, 127.4, 128.5, 130.3, 134.6, 146.2, 148.6 (Ar−C), 153.4 (C−═C), 160.3 (C═O), 166.7 (C−O), 167.4 (C−N), 193.5 (C═O). MS (*m/z*, (relative abundance, %)): 464 (M^{+1}, 8), 342 (100), 182 (54), 162 (37), 123 (15).

4-hydroxy-8-(5-(3-(4-hydroxyphenyl)acryloyl)-6-methyl-2-thioxo-1,2,3,4-tetrahydro pyrimidin4-yl)-2H-chromen-2-one (DCCT 5). Reddish Brown solid; yield 69.56%; m.p. 176–178 °C; IR (KBr, cm^{-1}): v 3437(O−H), 3295(N−H), 3021(C−H Ar), 2942(C−H), 1679(C═O), 1605 (C═C), 1282, 1055 (C−O) 752 (o-sub); ^{1}H NMR (400 MHz, DMSO-d_6, δ/ppm): 2.37(s, 3H, CH), 4.77(s, H, CH, Ar), 5.26 (s, H, OH), 6.02 (s, 2H, NH), 6.55–7.25 (m, 8H, Ar), 7.60 (d, 2H, CH═CH), 9.58 (s, H, OH). ^{13}C NMR (100 MHz, DMSO-d_6) δ/ppm: 18.36 (CH_3), 45.6(C−CH), 91.3, 115.8, 116.4, 117.6, 124.7, 125.2, 126.1, 127.6, 128.3, 130.4, 148.4 (Ar−C), 152.2 (C═C), 157.8.1, 166.1 (C−OH), 161.7 (C═O), 167.4 (C−N), 174.7 (C═S) 193.5 (C═O). MS (*m/z*, (relative abundance, %)): 435 (M^{+1}, 12), 342 (26), 182 (100), 162 (33), 94 (54).

4-hydroxy-8-(6-methyl-5-(3-(4-nitrophenyl)acryloyl)-2-thioxo-1,2,3,4-tetrahydro pyrimidin4-yl)-2H-chromen-2-one (DCCT 6). Brown solid; yield 63.42%; m.p. 255–257 °C; IR (KBr, cm^{-1}): v 3454 (O−H), 3297(N−H), 3048(C−H Ar), 2915(C−H), 1675(C═O), 1603 (C═C),1532, 1326 (Nitro), 1289 (C−O), 762 (o-sub); ^{1}H NMR (400 MHz, DMSO-d_6, δ/ppm): 2.42 (s, 3H, CH), 4.91(s, H, CH), 6.10 (s, 2H, NH), 6.80–7.74 (m, 8H, Ar), 8.20(d, 2H, C═C), 9.74 (s, H, OH). ^{13}C NMR (100 MHz, DMSO-d_6) δ/ppm: 17.8 (CH_3), 44.7(C−CH), 91.8, 116.2, 117.5, 121.6, 124.8, 125.2, 126.2, 127.5, 128.9, 141.5, 146.2, 148.3, (Ar−C), 152.6 (C═C), 160.1 (C═O), 166.6 (C−O), 168.4 (C−N), 193.2 (C═O). MS (*m/z*, (relative abundance, %)): 464 (M^{+1}, 8), 344 (58), 182 (100), 162 (24), 123 (31).

8-(5-(3-(4-chlorophenyl)acryloyl)-6-methyl-2-thioxo-1,2,3,4-tetrahydropyrimidin4-yl)-4-hydroxy-2H-chromen-2-one (DCCT 7). Golden yellow solid; yield 56.75%; m.p. 170–172 °C; IR (KBr, cm^{-1}): v 3405(O−H), 3265(N−H), 3019(C−H Ar), 2942(C−H), 1682(C═O), 1614 (C═C), 1289 (C−O) 751 (o-sub); ^{1}H NMR (400 MHz, DMSO-d_6, δ/ppm): 2.39 (s, 3H, CH), 4.80 (s, H, CH), 6.16 (s, 2H, NH), 6.80–7.30 (m, 8H, Ar), 7.74(d, 2H, CH═CH), 9.31 (s, H, OH). ^{13}C NMR (100 MHz,

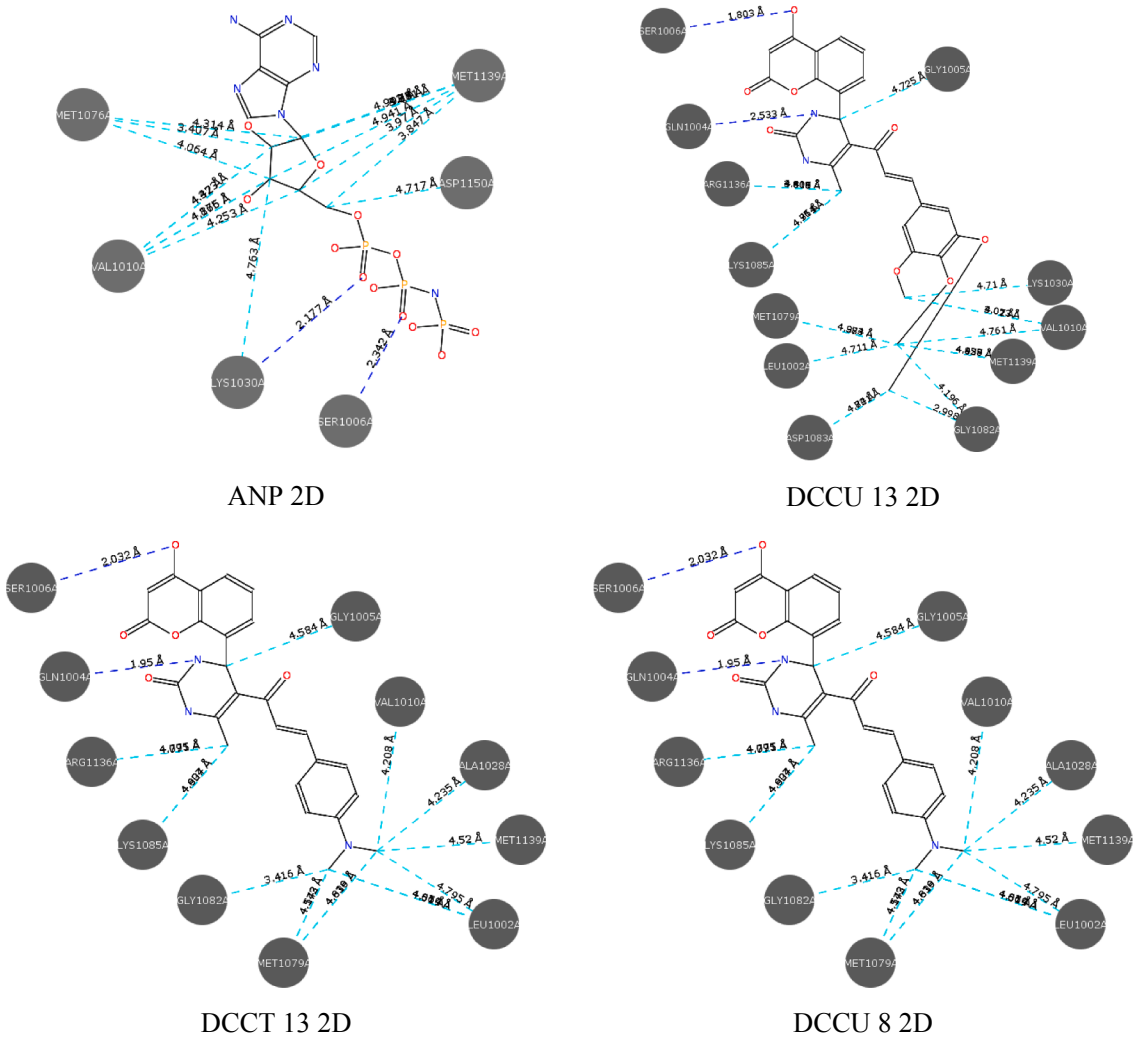

Fig. 1. Interactions of hybrids against Insulin receptor (1IR3) in 2D view.

DMSO-d_6) δ/ppm: 16.3 (CH_3), 40.6 (C−CH), 91.6, 116.4, 117.9, 124.6, 125.2, 126.7, 127.4, 128.8, 133.8, (Ar−C), 152.7 (CH═CH), 160.4 (C═O), 166.4 (C−O), 167.2 (C−N), 174.2 (C═S), 193.3 (C═O). MS (*m/z*, (relative abundance, %)): 453 (M^{+1}, 12), 342 (27), 182 (100), 162 (38), 112 (62).

8-(5-(3-(4-(dimethylamino)phenyl)acryloyl)-6-methyl-2-thioxo-1,2,3,4-tetrahydro pyrimidin4-yl)-4-hydroxy-2H-chromen-2-one (DCCT 8). Dark brown solid; yield 74.25%; m.p. 159–161 °C; IR (KBr, cm^{-1}): v 3416 (O−H), 3238(N−H), 2920(C−H Ar), 2850(C−H), 1649(C═O), 1599(C═C), 1273, 1042 (C−O), 768(p-sub); ^{1}H NMR (400 MHz, DMSO-d_6, δ/ppm): 2.45 (s, 3H, CH), 2.94 (s, 6H, CH), 5.10 (s, H, CH), 6.35 (s, 2H, NH), 6.55–7.15 (m, 8H, Ar),7.70 (d, 2H, CH═CH), 9.11 (s, H, OH). ^{13}C NMR (100 MHz, DMSO-d_6) δ/ppm: 20.7 (CH_3), 40. 2 (*N*−CH), 45.1 (C−CH), 92.5, 117.6, 118.2, 121.7, 123.4, 124.4, 125.1, 126.5, 128.7 (Ar−C), 148.4, 167.2 (Ar−C−N), 160.8 (C═O), 166.6 (C−O), 152.7 (C═C), 174.2 (C═S), 193.3 (C═O). MS (*m/z*, (relative abundance, %)): 442 (M^{+1}, 9), 342 (34), 182 (100), 162 (17), 121 (51).

4-hydroxy-8-(5-(3-(2-hydroxyphenyl)acryloyl)-6-methyl-2-thioxo-1,2,3,4-tetrahydro pyrimidin4-yl)-2H-chromen-2-one (DCCT 9). Orange solid; yield 58.37%; m.p. 176–178 °C; IR (KBr, cm^{-1}): v 3437(O−H), 3251(N−H), 2922(C−H Ar), 2851(C−H), 1688(C═O), 1610 (C═C), 1232(C−O), 754(o-sub); ^{1}H NMR (400 MHz, DMSO-d_6, δ/ppm): 2.53 (s, 3H, CH), 4.91 (s, H, CH), 5.24(s, H, OH), 6.42 (s, 2H, NH), 6.55–7.20 (m, 8H, Ar), 7.39 (d, 2H, CH═CH), 9.10 (s, H, OH). ^{13}C NMR (100 MHz, DMSO-d_6) δ/ppm: 16.8 (CH_3), 45.1 (C−CH), 91.7, 115.2, 116.5, 117.8, 124.7, 125.3, 126.5, 128.4, 129.8, 148.1 (Ar−C), 158.3, 162.7 (Ar−C−O), 160.3 (C═O), 167.3 (C−N), 174.3 (C═S), 193.4 (C═O). MS (*m/z*, (relative abundance, %)): 435 (M^{+1}, 11), 342 (55), 275 (100), 162 (23), 94 (47).

4-hydroxy-8-(5-(3-(3-hydroxyphenyl)acryloyl)-6-methyl-2-thioxo-1,2,3,4-tetrahydro pyrimidin4-yl)-2H-chromen-2-one (DCCT 10). Yellow solid; yield 64.79%; m.p. 175–177 °C; IR (KBr, cm^{-1}): v 3437(O−H), 3158(N−H), 3011(C−H Ar), 2892(C−H), 1692(C═O), 1472 (C═C), 1275(C−O), 754(m-sub); ^{1}H NMR (400 MHz, DMSO-d_6, δ/ppm): 2.30 (s, 3H, CH), 4.71 (s, H, CH), 5.38 (s, H, OH), 6.14 (s, 2H, NH), 6.65–7.10 (m, 8H, Ar), 7.69 (d, 2H, CH═CH), 9.52 (s, H, OH). ^{13}C NMR (100 MHz, DMSO-d_6) δ/ppm: 18.7 (CH_3), 42.8 (C−CH), 91.5, 112.3, 115.8, 116.2, 117.2, 119.3, 124.3, 125.6, 126.4, 128.4, 130.7, 136.2, 148.6 (Ar−C), 152. 8 (CH═CH), 158.7, 166.3 (C−O), 160.6 (C═O), 167.8 (C−N), 174.5 (C═S), 193.4 (C═O). MS (*m/z*, (relative abundance, %)): 435 (M+, 9), 342 (37), 274 (100), 162 (52), 94 (15).

4-hydroxy-8-(6-methyl-5-(3-(3-nitrophenyl)acryloyl)-2-thioxo-1,2,3,4-tetrahydro pyrimidin4-yl)-2H-chromen-2-one (DCCT 11). Greenish white solid; yield 59.42%; m.p. 149–151 °C; IR (KBr, cm^{-1}): v 3399(O−H), 3264(N−H), 3036(C−H Ar), 2944(C−H), 1688(C═O), 1489(C═C),1344 (Nitro), 1282 (C−O), 757(m-sub); ^{1}H NMR (400 MHz, DMSO-d_6, δ/ppm): 2.47 (s, 3H, CH), 4.72 (s, H, CH), 6.17 (s, 2H, NH), 6.80–7.62 (m, 8H, Ar), 8.30 (d, 2H, C═C), 9.88 (s, H, OH). ^{13}C NMR (100 MHz, DMSO-d_6) δ/ppm: 16.3 (CH_3), 43.6 (C−CH), 91.8,

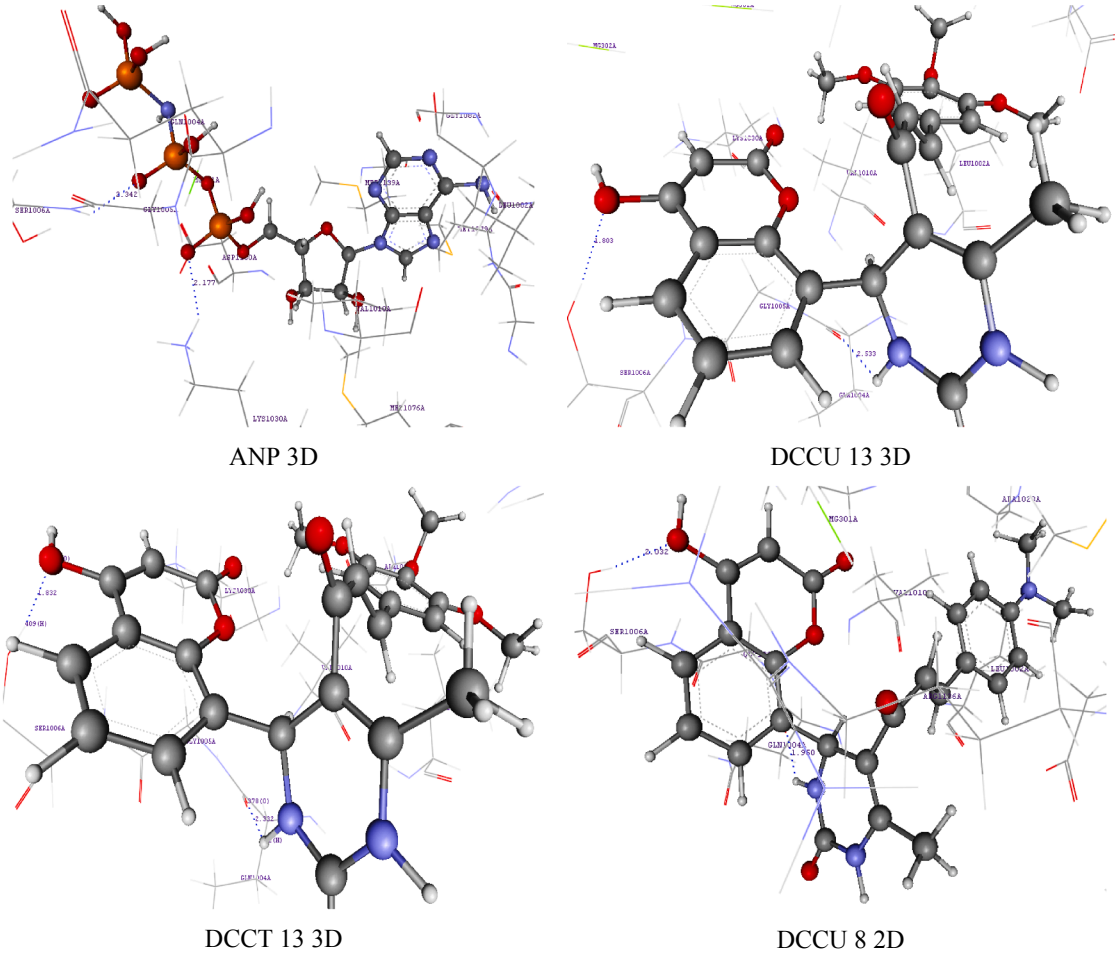

Fig. 2a. H-Bond Interactions of hybrids against Insulin receptor (1IR3) in 3D view.

116.3, 117.9, 120.3, 121.8, 124.1, 125.4, 126.7, 128.6, 129.9, 132.4, 136.5, 148.2 (Ar–C), 147.5, 152.6 (CH=CH), 160.2 (C=O), 165.3 (C–O), 167.8 (C–N), 174.7 (C=S), 193.2 (C=O). MS (*m/z*, (relative abundance, %)): 464 (M^{+1}, 11), 342 (55), 303 (100), 177 (38), 123 (21).

8-(5-(3-(2-chlorophenyl)acryloyl)-6-methyl-2-thioxo-1,2,3,4-tetrahydropyrimidin4-yl)-4-hydroxy-2H-chromen-2-one (DCCT 12). Brown solid; yield 64.62%; m.p. 137–139 °C; IR (KBr, cm^{-1}): v 3414(O–H), 3245(N–H), 3046(C–H Ar), 2938(C–H), 1688(C=O), 1602 (C=C), 1284(C–O), 752(p-sub); ^{1}H NMR (400 MHz, DMSO-d_6, δ/ppm): 2.35 (s, 3H, CH), 4.68 (s, H, CH), 6.11 (s, 2H, NH), 6.85–8.30 (m, 8H, Ar), 7.92 (d, 2H, CH=CH), 9.82 (s, H, OH). ^{13}C NMR (100 MHz, DMSO-d_6) δ/ppm: 18.3.2 (CH_3), 41.7 (C–CH), 91.2, 116.3, 117.5, 124.1, 125.6, 126.8, 127.5, 128.2, 129.6, 131.2, 133.6, (Ar–C), 152.7 (CH=CH), 160.5 (C=O), 166.6 (C–O), 167.8 (C–N) 174.8 (C=S), 193.5 (C=O). MS (*m/z*, (relative abundance, %)): 453 (M^{+2}, 14), 342 (31), 292 (100), 162 (61), 112 (26).

4-hydroxy-8-(6-methyl-2-thioxo-5-(3-(3,4,5-trimethoxyphenyl) acryloyl)-1,2,3,4-tetrahydropyrimidin4-yl)-2H-chromen-2-one (DCCT 13). Brick red solid; yield 73.88%; m.p. 216–218 °C; IR (KBr, cm^{-1}): v 3426(O–H), 3291(N–H), 2938(C–H Ar), 2840(C–H), 1696(C=O), 1596, 1478 (C=C), 1289, 1054(C–O), 754, 641(3,4,5-sub); ^{1}H NMR (400 MHz, DMSO-d_6, δ/ppm): 2.45 (s, 3H, CH), 3.75 (s, 9H, CH), 4.93 (s, H, CH), 6.32 (s, 2H, NH), 6.60–7.10 (m, 6H, Ar), 7.75 (d, 2H, CH=CH), 9.29 (s, H, OH). ^{13}C NMR (100 MHz, DMSO-d_6) δ/ppm: 16.3 (CH_3), 42.8 (C–CH), 56.8, (O–CH_3), 91.7, 103.9, 116.7, 117.2, 124.2, 125.1, 126.6, 128.9, 129.7, 148.2 (Ar–C), 150.5 (C-OCH_3), 152.4 (CH=CH), 160.3 (C=O), 166.1 (C–O),167.5 (C–N), 174.8 (C=S), 193.2 (C=O). MS (*m/z*, (relative abundance, %)): 509 (M^{+1}, 14), 342 (34), 182 (100), 162 (59), 168 (19).

3.2. In silico docking studies

The docking process against Insulin receptor (PDB ID: 1IR3) was validated by re-docking the co-crystal ligand and the RMSD values were calculated (Table 1). The docking results of coumarin-chalcone hybrids as ligands against Insulin receptor (PDB ID: 1IR3) includes that the docking scores (Table 2) of coumarin-chalcone hybrids DCCU 13, DCCT 13 and DUUC 8 showed the least binding score of −83.15, −82.72 and −82.26 respectively, among all the coumarin-chalcone hybrids when compared to internal ligand (ANP) and standard drug metformin having docking score of −68.64 and −24.57 respectively, which indicates that hybrids DCCU 13, DCCT 13 and DUUC 8 has a higher binding affinity to the amino acid residues at the active pocket of Insulin receptor protein. The interactions of the ligands against the target protein (Figs. 1, 2a, and 2b) were compared with that of interactions of internal ligand ANP against the target protein. The ANP has the Hydrophobic interactions with LEU 1002, GLY 1003, GLN 1004, GLY 1005, VAL 1010, ALA 1028, MET 1076, LEU 1078, MET 1079, GLY 1082 ASP 1083, and MET 1139. The least scored hybrids interact with protein residues SER1006 and GLN1004 through H-bond, LEU 1002, GLN 1004, GLY 1005, SER 1006, VAL 1010, LYS 1030, MET 1079, GLY 1082 ASP 1083, LSY 1085, ARG 1136, and MET 1139 through hydrophobic and Van der Waal interactions.

3.3. Acute oral toxicity studies

Molecules were tested for acute oral toxicity *in vivo*; findings showed

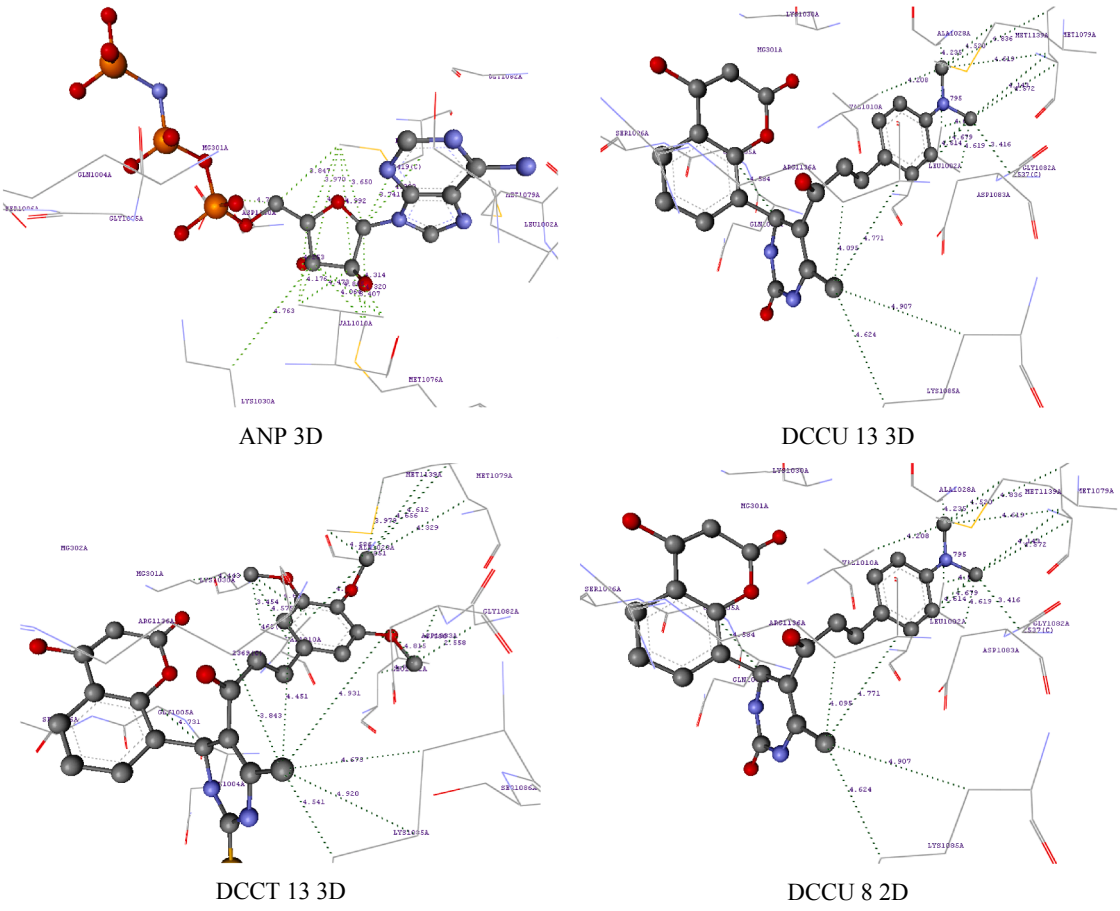

Fig. 2b. Hydrophobic Interactions of hybrids against Insulin receptor (1IR3) in 3D view.

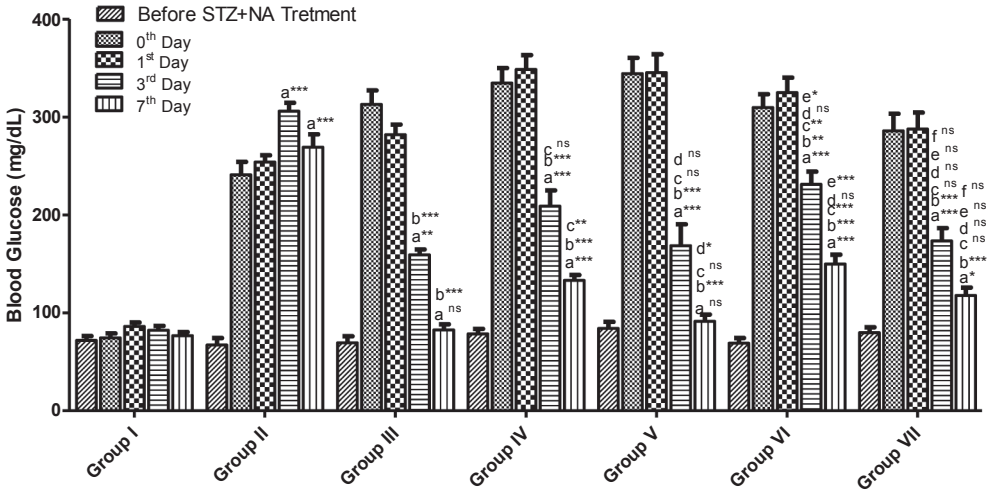

Fig. 3. Effect of DCCU 13 and DCCT 13 on fasting blood glucose (mg/dL) in STZ + NA induced diabetic rats. All data are expressed as Mean ± SEM (n = 6), Comparison: All groups: a – compared Group I; b – compared with Group II; c – compared with Group III; d-compared with Group IV; e – compared with Group V; f – compared with Group VI. ***p ≤ 0.001, **p ≤ 0.01, *p ≤ 0.05 and ns = non-significant. Significance was measured using One-way ANOVA followed by Tukey's test.

that the 300 mg/kg dosage of molecules was healthy, proof of no significant alterations in body weight, behavioral changes, and abnormal breathing. Further confirmed by no signs of morbidity or mortality and adverse effects were observed in treated animals over the next 14 days of treatment. So the 300 mg/kg body weight of animal dose was considered as a safe dose and further 2000 mg/kg dose was not tested due to heaver in dose.

3.4. In vivo anti-diabetic evaluation

The single dose intra-peritoneal administration of STZ (60 mg/kg body weight) after 20 min of nicotinamide (110 mg/kg body weight) administration through intra-peritoneal route to selected animal groups leads to development of type 2 diabetes mellitus. The animals with BGL more than 180 mg/dL considered as diabetic rats and were included into anti-diabetic screening. The hybrids DCCU 13 and DCCT 13 were more affine towards the insulin protein through *in silico* studies, the

Table 3
Effect of DCCU 13 and DCCT 13 on fasting blood glucose (mg/dL) in STZ + NA induced diabetes rats.

S. No.	Group No	Treatment	Fasting blood glucose (mg/dL) (Mean ± SEM)				
			Before STZ-NA Treatment	0th Day	1st Day	3rd Day	7th Day
1	Group I	Normal Control	71.83 ± 4.52	74.50 ± 4.46	86.16 ± 4.07	82.33 ± 4.50	76.83 ± 3.49
2	Group II	Diabetic Control	72.83 ± 5.40	241.00 ± 13.38	254.16 ± 6.96	306.16 ± 8.54 a***	269.16 ± 13.23 a***
3	Group III	Diabetic + Metformin (100 mg/kg)	72.00 ± 5.88	313.00 ± 14.36	282.00 ± 10.53	159.33 ± 5.48 a**, b***	82.66 ± 5.67 a ^{ns}, b***
4	Group IV	Diabetic + DCCU 13 (15 mg/kg)	67.83 ± 5.30	334.83 ± 15.22	348.66 ± 14.64	209.16 ± 15.99 a***, b***, c^{ns}	133.16 ± 5.65 a***, b***, c**
5	Group V	Diabetic + DCCU 13 (30 mg/kg)	84.16 ± 6.58	344.50 ± 16.09	345.50 ± 18.75	168.66 ± 21.89 a***, b***, c^{ns}, d ^{ns}	91.50 ± 6.90 a ^{ns}, b***, c ^{ns}, d*
6	Group VI	Diabetic + DCCT 13 (15 mg/kg)	69.00 ± 5.22	309.83 ± 13.53	325.16 ± 15.26	231.33 ± 12.94 a***, b**, c**, d ^{ns}, e*	150.00 ± 9.60 a***, b***, c***, d^{ns}, e***
7	Group VII	Diabetic + DCCT 13 30 (mg/kg)	79.83 ± 5.56	286.00 ± 17.37	287.83 ± 16.80	173.66 ± 12.90 a***, b***, c^{ns}, d ^{ns}, e ^{ns}, f ^{ns}	117.83 ± 8.05 a*, b**, c ^{ns}, d ^{ns}, e^{ns}, f ^{ns}

All data are expressed as Mean ± SEM (n = 6), Comparison: All groups: a – compared Group I; b – compared with Group II; c – compared with Group III; d-compared with Group IV; e – compared with Group V; f – compared with Group VI. ***p ≤ 0.001, **p ≤ 0.01, *p ≤ 0.05, ns = non-significant. Significance was measured using One-way ANOVA followed by the Tukey's test.

Table 4
Effect of DCCU 13 and DCCT 13 on body weight (gm) in STZ + NA induced diabetic rats.

S. No.	Group	Treatment	Bodyweight (gm) (Mean ± SEM)				
			Before Treatment	0th Day	1st Day	3rd Day	7th Day
1	Group I	Normal Control	177.66 ± 4.64	178.66 ± 4.58	180.66 ± 4.81	182.16 ± 4.79	183.83 ± 4.77
2	Group II	Diabetic Control	163.00 ± 4.95	154.83 ± 4.89	153.50 ± 5.06	151.33 ± 5.04 a***	148.83 ± 5.10 a***
3	Group III	Diabetic + Metformin (100 mg/k)	169.16 ± 3.02	157.33 ± 3.07	155.50 ± 2.83	152.33 ± 2.64 a**, b ^{ns}	149.66 ± 2.62 a***, b ^{ns}
4	Group IV	Diabetic + DCCU 13 (15 mg/kg)	164.16 ± 4.75	158.33 ± 4.77	156.16 ± 4.73	149.50 ± 2.07 a***, b ^{ns}, c ^{ns}	148.00 ± 2.01 a***, b ^{ns}, c ^{ns}
5	Group V	Diabetic + DCCU 13 (30 mg/kg)	190.50 ± 5.85	182.16 ± 6.26	183.66 ± 6.01	188.00 ± 6.00 a ^{ns}, b***, c***, d***	191.50 ± 5.53 a ^{ns}, b***, c***, d***
6	Group VI	Diabetic + DCCT 13 (15 mg/kg)	178.00 ± 6.12	168.00 ± 6.15	168.16 ± 6.64	170.00 ± 6.59 a ^{ns}, b ^{ns}, c ^{ns}, d ^{ns}, e ^{ns}	171.16 ± 6.35 a ^{ns}, b*, c*, d*, e*
7	Group VII	Diabetic + DCCT 13 (30 mg/kg)	178.66 ± 3.62	169.00 ± 3.94	171.83 ± 3.84	174.50 ± 3.67 a ns, b *, c*, d**, e ^{ns}, f^{ns}	176.33 ± 3.67 a ^{ns}, b**, c**, d**, e ^{ns}, f ^{ns}

All data are expressed as Mean ± SEM (n = 6), Comparison: All groups a – compared Group I; b – compared with Group II; c – compared with Group III; d – compared with Group IV; e – compared with Group V; f – compared with Group VI. ***p ≤ 0.001, **p ≤ 0.01, *p ≤ 0.05, ns = non-significant. Significance was measured using One-way ANOVA followed by the Tukey's test.

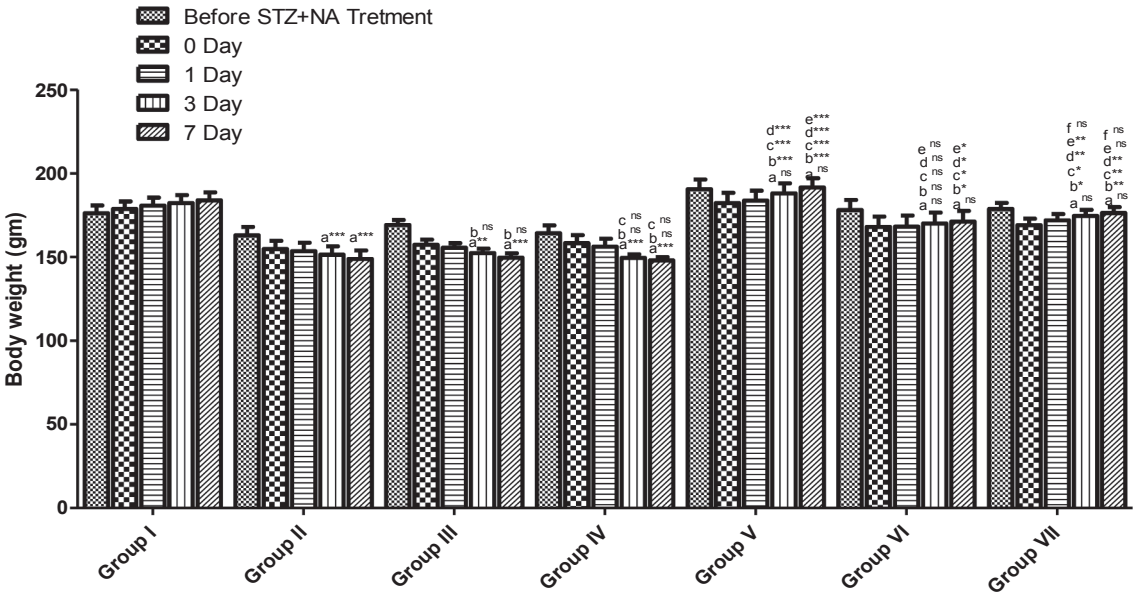

Fig. 4. Effect of DCCU 13 and DCCT 13 on body weight (gm) in STZ + NA induced diabetic rats. All data are expressed as Mean ± SEM (n = 6), Comparison: All groups a – compared Group I; b – compared with Group II; c – compared with Group III; d-compared with Group IV; e – compared with Group V; f – compared with Group VI. ***p ≤ 0.001, **p ≤ 0.01, *p ≤ 0.05, ns = Non-significant. Significance was measured using One-way ANOVA followed by the Tukey's test.

same hybrids in low and high (15 mg/kg and 30 mg/kg respectively) doses were screened for *in vivo* anti-diabetic activity in STZ + NA induced type 2 diabetic rats. The anti-diabetic activity of the hybrids were evaluated by determination of fasting blood glucose level (BGL), change in body weight, oxidative stress related parameters (MDA, SOD and GSH) and histopathological changes in liver and pancreas tissues.

3.4.1. Blood glucose level (BGL) analysis

The fasting BGL of normal and diabetic, and diabetic treated animal groups were measured by digital glucometer at before STZ + NA treatment, 0th, and at the end of 1st, 3rd, and 7th day after the treatment with standard and test drugs by collecting drop of blood at tip of tail through tiny puncture with sterile needle. Significantly elevated fasting BGL was observed in STZ + NA (Group II) induced diabetic animals than fasting BGL in normal animals (Group I) at the end of 3rd and 7th day of study protocol (Fig. 3, Table 3). In contrast the significant decrease in fasting BGL was found at the end of 3rd and 7th day study period in diabetic animals treated with 100 mg/kg body weight b.d. dose of metformin (Group III) and 15 and 30 mg/kg body weight b.d. dose of DCCU 13 (Group IV and group V) and DCCT 13 (Group VI and Group VII) treatment when compared to fasting BGL of diabetic control group animals. Further, no significant difference in fasting BGL between metformin and 15 and 30 mg/kg dose of DCCU 13 (Group IV and group V) and 30 mg/kg dose of DCCT 13 (Group VII) was found at the end of 3rd day and 30 mg/kg dose of DCCU 13 and DCCT 13 at the end of the 7th day study period. Among all the treatment groups 30 mg/kg dose of DCCU 13 (Group V) and DCCT 13 (Group VII) showed better protection against STZ + NA increased BGL in animals.

3.4.2. Bodyweight analysis

The significant decrease in body weight of STZ + NA (Group II) induced type 2 diabetic animal groups was observed when compared to body weight of normal animals (Group I). Further, significant decrease of body weight was observed in metformin 100 mg/kg (Group III) body weight b.d. dose treated group animals for about 7 days when compared to normal control (Group I) and even diabetic control group animals (Group II). The significant increment in body weight was observed in animal groups treated with 30 mg/kg body weight b.d. dose of DCCU 13 (Group V, ***p < 0.001) and DCCT 13 (Group VII, *p < 0.05) for about 3rd day and on 7th day 15 mg/kg (Group VI, *p < 0.05) and 30 mg/kg (Group VII, **p < 0.01) body weight b.d. dose of DCCT 13 and 30 mg/kg (Group V, ***p < 0.001) body weight b.d. dose of DCCU 13 showed significant increased body weight when compared to body weight of diabetic control group animals and metformin treatment group. Among all the groups DCCU 13 at 30 mg/kg body weight b.d. dose showed better effect against STZ + NA induced attenuation in body weight (Table 4, Fig. 4).

3.4.3. Estimation of oxidative stress biomarkers

3.4.3.1. Estimation of oxidative stress biomarkers in pancreas tissue. A significant increase in lipid peroxidation (MDA) and a decrease in SOD and GSH levels were observed in pancreas tissue of diabetic control group (Group II) when compared to the control group (Group I). While the treatment of diabetic animals with metformin (p.o) (Group III), DCCU 13 (Group V) and DCCT13 (Group VII) at 30 mg/kg b.d doses (p.o) showed a significant reduction in lipid peroxidation and increased SOD & GSH when compared to the diabetic control group. Oral administration of 30 mg/kg b.d dose of DCCU 13 (Group V) and DCCT13 (Group VII) showed a significant change in the STZ + NA induced alterations in oxidative stress biomarkers when compared to low dose (15 mg/kg b.d dose) (Table 5 and Figs. 5–7).

3.4.3.2. Estimation of oxidative stress biomarkers in liver tissue. The diabetic control group (Group II) showed a significant increase in lipid peroxidation in the liver tissue when compared to the control animal group (Group I). Whereas treated diabetic animal groups with metformin (p.o) (Group III), DCCU 13 (Group V) and DCCT13 (Group VII) at 30 mg/kg b.d doses (p.o) showed attenuation in the malondialdehyde level which was significant with the diabetic control group. High dose 30 mg/kg b.d dose of DCCU 13 (Group V) and DCCT13 (Group VII) showed a significant reduction in MDA and increased SOD & GSH when compared to low dose (15 mg/kg b.d dose) (Table 5 and Figs. 8–10).

3.4.4. Histopathology

Histopathological examinations, there were no remarkable alterations in the pancreatic architecture observed in normal, whereas shrunken β-islet cells, cell necrosis, and vacuolization of cytoplasm

Table 5
Effect of DCCU 13 and DCCT 13 on SOD, GSH and MDA in Pancreatic and liver tissue of STZ + NA induced diabetic rats.

S. No.	Group	Treatment	MDA (nM/gm wet tissue)		SOD (U/gm wet tissue)		GSH (μM/gm wet tissue)	
			Pancreatic	Liver	Pancreatic	Liver	Pancreatic	Liver
1	Group I	Normal Control	9.86 ± 0.50	10.35 ± 0.60	76.28 ± 2.85	57.23 ± 3.00	8.32 ± 0.64	4.89 ± 0.41
2	Group II	Diabetic Control	29.47 ± 1.45 a^{***}	36.52 ± 0.37 a^{***}	20.33 ± 1.09 a^{***}	27.72 ± 4.40 a^{***}	2.08 ± 0.64 a^{***}	0.55 ± 0.22 a^{***}
3	Group III	Diabetic + Metformin (100 mg/k)	12.41 ± 0.62 a^{ns}, b^{***}	12.71 ± 0.93 a^{ns}, b^{***}	68.89 ± 1.95 a^{ns}, b^{***}	53.81 ± 2.85 a^{ns}, b^{***}	7.75 ± 0.50 a^{ns}, b^{***}	4.14 ± 0.14 a^{ns}, b^{***}
4	Group IV	Diabetic + DCCU 13 (15 mg/kg)	18.90 ± 0.80 a^{***}, b^{**}, c^{***}	20.13 ± 0.57 a^{***}, b^{***}, c^{***}	53.42 ± 1.71 a^{***}, b^{***}, c^{***}	30.50 ± 2.33 a^{***}, b^{ns}, c^{***}	3.88 ± 0.34 a^{***}, b^{ns}, c^{***}	2.05 ± 0.16 a^{***}, b^{ns}, c^{***}
5	Group V	Diabetic + DCCU 13 (30 mg/kg)	13.39 ± 0.53 a^{ns}, b^{***}, c^{ns}, d^{***}	13.74 ± 0.83 a^{ns}, b^{***}, c^{ns}, d^{***}	68.04 ± 1.51 a^{ns}, b^{***}, c^{ns}, d^{***}	50.89 ± 0.86 a^{ns}, b^{***}, c^{ns}, d^{**}	7.41 ± 0.28 a^{ns}, b^{***}, c^{ns}, d^{***}	4.11 ± 0.08 a^{ns}, b^{***}, c^{ns}, d^{**}
6	Group VI	Diabetic + DCCT 13 (15 mg/kg)	23.61 ± 0.66 a^{***}, b^{ns}, c^{***}, d^{ns}, e^{***}	24.29 ± 0.73 a^{***}, b^{***}, c^{***}, d^{*}, e^{***}	41.12 ± 0.68 a^{***}, b^{***}, c^{***}, d^{**}, e^{***}	25.93 ± 3.00 a^{***}, b^{ns}, c^{***}, d^{ns}, e^{***}	3.50 ± 0.14 a^{***}, b^{ns}, c^{***}, d^{ns}, e^{***}	1.43 ± 0.24 a^{***}, b^{ns}, c^{***}, d^{ns}, e^{***}
7	Group VII	Diabetic + DCCT 13 (30 mg/kg)	15.63 ± 0.54 a^{*}, b^{***}, c^{ns}, d^{**}, e^{ns}, f^{***}	16.48 ± 0.74 a^{***}, b^{***}, c^{*}, d^{*}, e^{ns}, f^{***}	51.55 ± 2.28 a^{**}, b^{***}, c^{ns}, d^{*}, e^{ns}, f^{***}	43.16 ± 2.33 a^{*}, b^{***}, c^{ns}, d^{ns}, e^{ns}, f^{**}	6.33 ± 0.26 a^{ns}, b^{***}, c^{ns}, d^{*}, e^{ns}, f^{**}	3.59 ± 0.16 a^{*}, b^{***}, c^{ns}, d^{ns}, e^{ns}, f^{*}

All data are expressed as Mean ± SEM (n = 6), Comparison: All groups a – compared with Group I, b – compared with Group II, c – compared with Group III, d – compared with Group IV, e – compared with Group V, f – compared with Group VI. $^{***}p \leq 0.001$, $^{**}p \leq 0.01$, $^{*}p \leq 0.05$ and ns = non-significant. Significance was measured by One-Way ANOVA followed by the Tukey's test.

were found in STZ + NA group. Diabetic rats treated with metformin, and Group V (30 mg/kg, b.d. dose of DCCU 13) showed protection against STZ + NA induced alterations in pancreatic structure. Further, in Group VII (30 mg/kg, b.d. dose of DCCT 13 showed partial protection of pancreatic tissue (Fig. 11).

Light microscopic findings of the liver of control group animals histology showed the hepatocytes with distinct cytoplasm, rounded nucleus arranged around the central vein canal, while the diabetic control group revealed the dilated hepatocytes with the absence of nuclei, irregular and dilated central vein canal, and increased vacuolization of hepatocyte cytoplasm. Diabetic rats treated with 100 mg/kg, b.d. dose of Metformin (Group III) and30 mg/kg, b.d. dose of DCCU 13 (Group V) .animals visualizing (Fig. 12) showed no major alterations in hepatocytes.

4. Discussion

A total of 54 coumarin-chalcone hybrids were synthesized by well-known Biginelli synthesis, Pechmann condensation, Acetylation, and Claisen-Schmidt reactions. The best percentage of final product yield was obtained from Biginelli condensation using citric acid synthesis compared to sulphuric acid [84]. Sethna et al. reported that malonic acid in the phosphorous oxychloride and zinc chloride mixture increased the final product of Pechmann condensation relative to the excess concentration of sulphuric acid [85].

The insulin receptor is a tyrosine kinase transmembrane receptor that is effectively involved in the regulation of glucose homeostasis (disturbance leading to diabetes mellitus, cancer, and other clinical conditions) in the human body by phosphorylation against insulin binding [86]. The Insulin receptor (PDB ID: 1IR3) is the potential target for the screening of insulin receptor activators for their anti-diabetic ligand activity [87]. Flavonoids can potentially enable the insulin receptor to maintain glucose homeostasis [88]. Pawan et al., [86] stated that the internal ligand (ANP) interacted with amino acid residues like SER 1006, LYS 1030, ASP 1083, MET 1079 and GLU 1077 and H-bond acceptor would affect the docking score, while the results of present work indicated that the internal ligand (ANP) of insulin protein showed interactions with LEU 1002, GLY 1003, GLN 1004, GLY 1005, VAL 1010, ALA 1028, MET 1076, LEU 1078, MET 1079, GLY 1082 ASP 1083, and MET 1139. Tharini et al. [89] reported that ligands forming more H-bonds with amino acid residues in the active pocket of 1IR3 protein have a strong affinity to insulin (1IR3) protein. The ligands forming H-bonds with the least docking score than the internal ligand are stated by different authors [90–94]. Results showed that the least valued hybrids have two hydrogen bonds with SER1006 and GLN1004 amino acid residues, whereas the internal standard does not form H-bond interactions with proteins. Jayasree et al.,[95] stated that 3,4,5 trimethoxy-substituted cinnamic acid and 2-chloro-substituted cinnamic acid had a high binding affinity, especially interacting with the active site residue SER1006, Similarly, the results indicate that the hybrids with the lowest docking values DCCU 13 and DCCT 13 have a 3,4,5 trimethoxy substitution on the B ring of the chalcone portion. Interaction of ligands with other amino acid residues that are prominent in the anti-diabetic behavior documented by different researchers are LEU1002, LYS1030, ASP 1047, GLU 1047, LEU 1061, LEU 1062, LEU 1063, GLU1077, MET1079, ASP1083, GLN 1107, ASN 1137, ARG 1131, ILE 1148, ASP 1150, PHE1151, LYS1165, LEU 1171, GLN 1208, and ASN 1215 [82–88]. Previous works reported that the interaction of ligands with amino acid residues of insulin protein through more H-bonds, increasing of H-bond acceptors, 3,4,5-trimethoxy substitution would improve the anti-diabetic activity. The *in silico* docking results of coumarin-chalcone hybrids against Insulin (1IR3) protein show that the hybrids DCCU 13, DCCT 13 and DUUC 8 showed lowest docking score, interacts with amino acid residues at active protein pocket via two H-bonds along with Hydrophobic, Van der Waals interactions and has 3,4,5 trimethoxy (DCCU 13, DCCT 13), p-NO_2 (DUUC 8) Substitution of

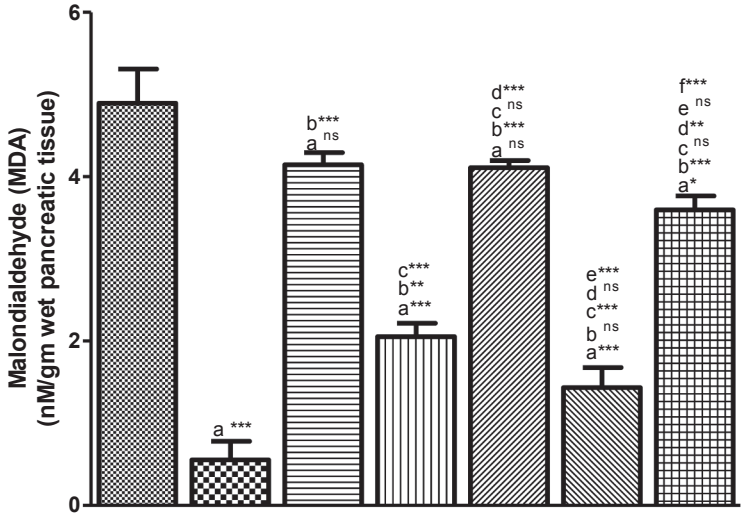

Fig. 5. Effect of DCCU 13 and DCCT 13 treatment on MDA in Pancreatic tissue of STZ + NA induced diabetic rats. All data are expressed as Mean ± SEM (n = 6), Comparison: All groups a-compared with Group I, b – compared with Group II, c – compared with Group III, d – compared with Group IV, e – compared with Group V, f – compared with Group VI. ***p ≤ 0.001, **p ≤ 0.01, *p ≤ 0.05 and ns = non-significant. Significance was measured by One-Way ANOVA followed by the Tukey's test.

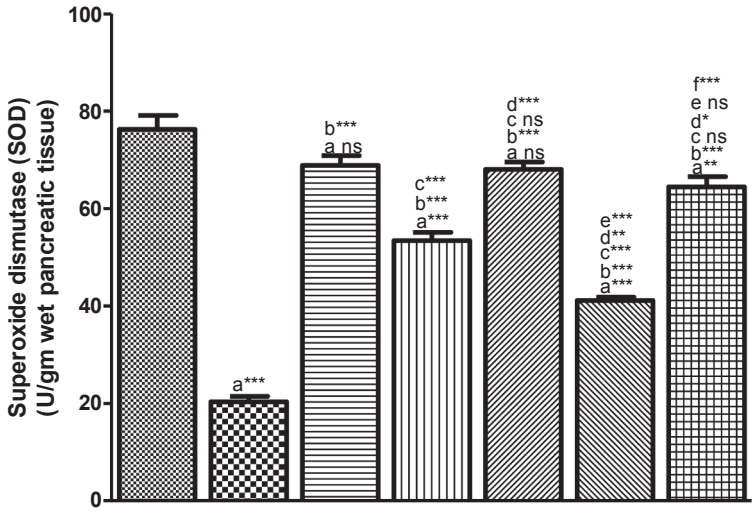

Fig. 6. Effect of DCCU 13 and DCCT 13 treatment on SOD in Pancreatic tissue of STZ + NA induced diabetic rats. All data are expressed as Mean ± SEM (n = 6), Comparison: All groups a-compared with Group I, b – compared with Group II, c – compared with Group III, d – compared with Group IV, e – compared with Group V, f – compared with Group VI. ***p ≤ 0.001, **p ≤ 0.01, *p ≤ 0.05 and ns = non-significant. Significance was measured by One-Way ANOVA followed by the Tukey's test.

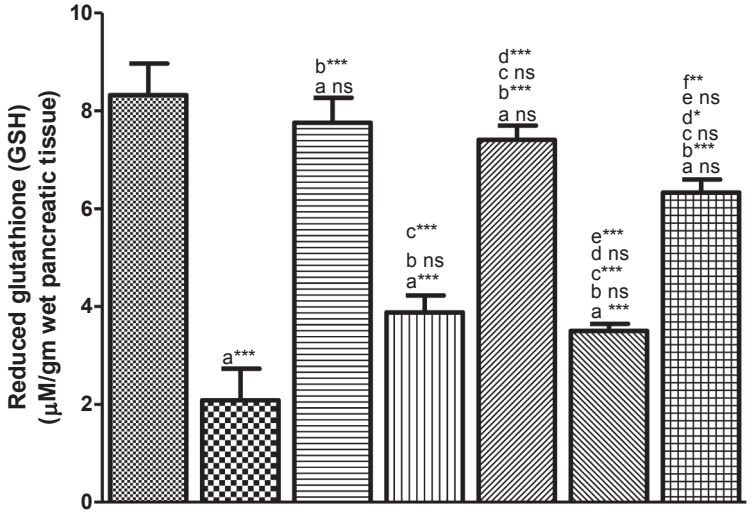

Fig. 7. Effect of DCCU 13 and DCCT 13 treatment on GSH in Pancreas tissue of STZ + NA induced diabetic rats. All data are expressed as Mean ± SEM (n = 6), Comparison: All groups a-compared with Group I, b – compared with Group II, c – compared with Group III, d – compared with Group IV, e – compared with Group V, f – compared with Group VI. ***p ≤ 0.001, **p ≤ 0.01, *p ≤ 0.05 and ns = non-significant. Significance was measured by One-Way ANOVA followed by the Tukey's test.

the chalcone part of the B ring which suggests that the findings were in line with previous results published by different research groups and may have shown anti-diabetic activity. More *in-vitro* and *in-vivo* studies are required to test their anti-diabetic activity.

The hybrids DCCU 13 and DCCT 13 which have 3,4,5-trimethoxy substitution on the phenyl ring of chalcone part attached to the dihydropyrimidinone ring at higher (30 mg/kg body weight) concentration showed a significant reduction in blood glucose, improved the weight loss associated with hyperglycemia, and repairing of STZ induced damage of liver and pancreatic β-lets. Considering these results, Kaushik

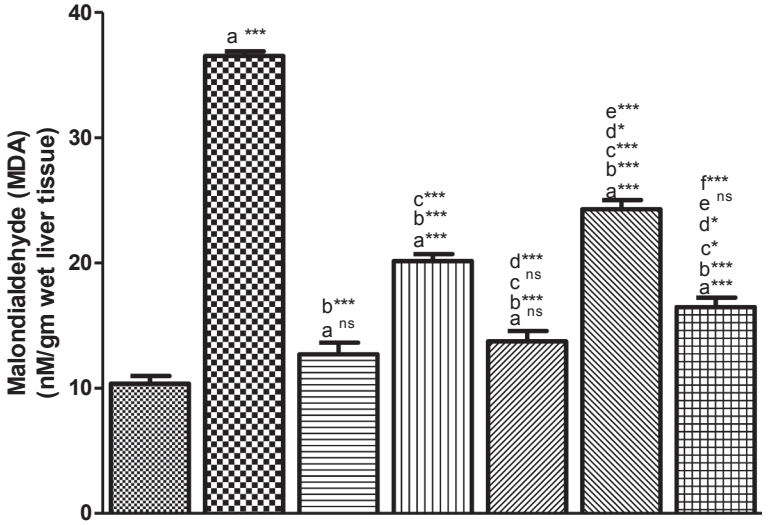

Fig. 8. Effect of DCCU 13 and DCCT 13 treatment on MDA in liver tissue of STZ + NA induced diabetic rats All data are expressed as Mean ± SEM (n = 6), Comparison: All groups a-compared with Group I, b – compared with Group II, c – compared with Group III, d – compared with Group IV, e – compared with Group V, f – compared with Group VI. ***p ≤ 0.001, **p ≤ 0.01, *p ≤ 0.05 and ns = non-significant. Significance was measured by One-Way ANOVA followed by the Tukey's test.

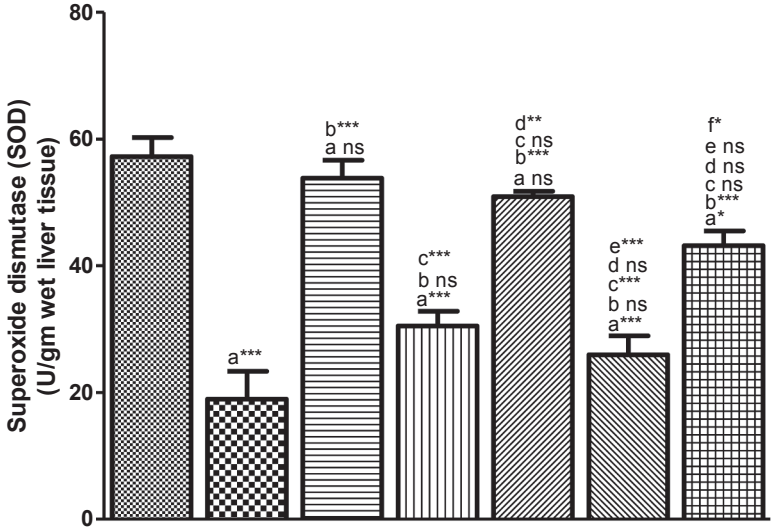

Fig. 9. Effect of DCCU 13 and DCCT 13 treatment on SOD in liver tissue of STZ + NA induced diabetic rats. All data are expressed as Mean ± SEM (n = 6), Comparison: All groups a-compared with Group I, b – compared with Group II, c – compared with Group III, d – compared with Group IV, e – compared with Group V, f – compared with Group VI. ***p ≤ 0.001, **p ≤ 0.01, *p ≤ 0.05 and ns = non-significant. Significance was measured by One-Way ANOVA followed by the Tukey's test.

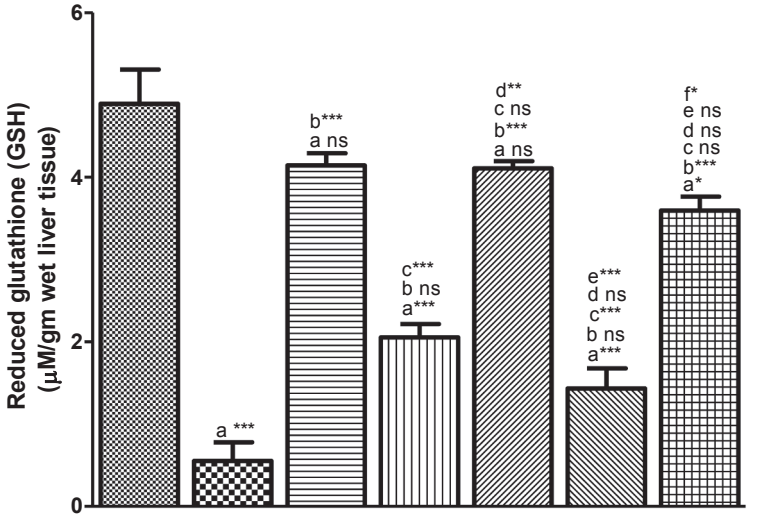

Fig. 10. Effect of DCCU 13 and DCCT 13 treatment on GSH in liver tissue of STZ + NA induced diabetic rats. All data are expressed as Mean ± SEM (n = 6), Comparison: All groups a-compared with Group I, b – compared with Group II, c – compared with Group III, d – compared with Group IV, e – compared with Group V, f – compared with Group VI. ***p ≤ 0.001, **p ≤ 0.01, *p ≤ 0.05 and ns = non-significant. Significance was measured by One-Way ANOVA followed by the Tukey's test.

et al. [96] stated that compounds with electron-donating groups at ortho, meta, and para-position or electron-removing groups at ortho or meta-position at the phenyl ring should have substantial anti-diabetic and anti-oxidant activity. Few researchers [97–99] indicated that the phenyl ring substitution of 3,4,5-trimethoxy is present in compounds responsible for the significant antidiabetic activity and for improving

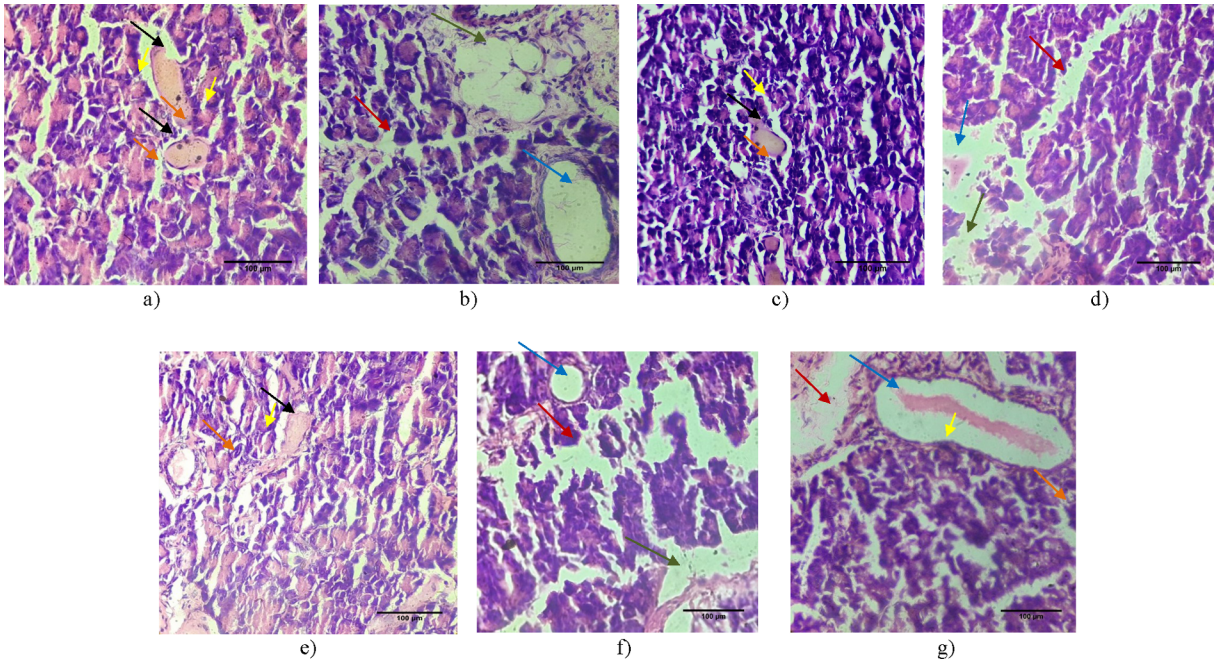

Fig. 11. Histology of pancreas in experimental rats after 7 days of treatment (H&E, 400×). (a) Group I: normal animals showed normal β-islet cells (black arrow), acinar cells (yellow arrow), blood sinusoids (orange arrow), (b) Group II: STZ + NA showed shrunken β-islet cells (blue arrow), cell necrosis (green arrow), vacuolization of cytoplasm (red arrow), (c) Group III: Metformin 100 mg/kg showed normal pancreatic architecture, (d) Group IV: DCCU 15 mg/kg showed damage of pancreatic tissue, (e) Group V: DCCU 30 mg/kg reverted the pancreatic damage, (f) Group VI: DCCT 15 mg/kg showed damage of pancreatic tissue, and (g) Group VII: DCCT 30 mg/kg showed partial protection of diabetic pancreatic tissue. (For interpretation of the references to colour in this figure legend, the reader is referred to the web version of this article.)

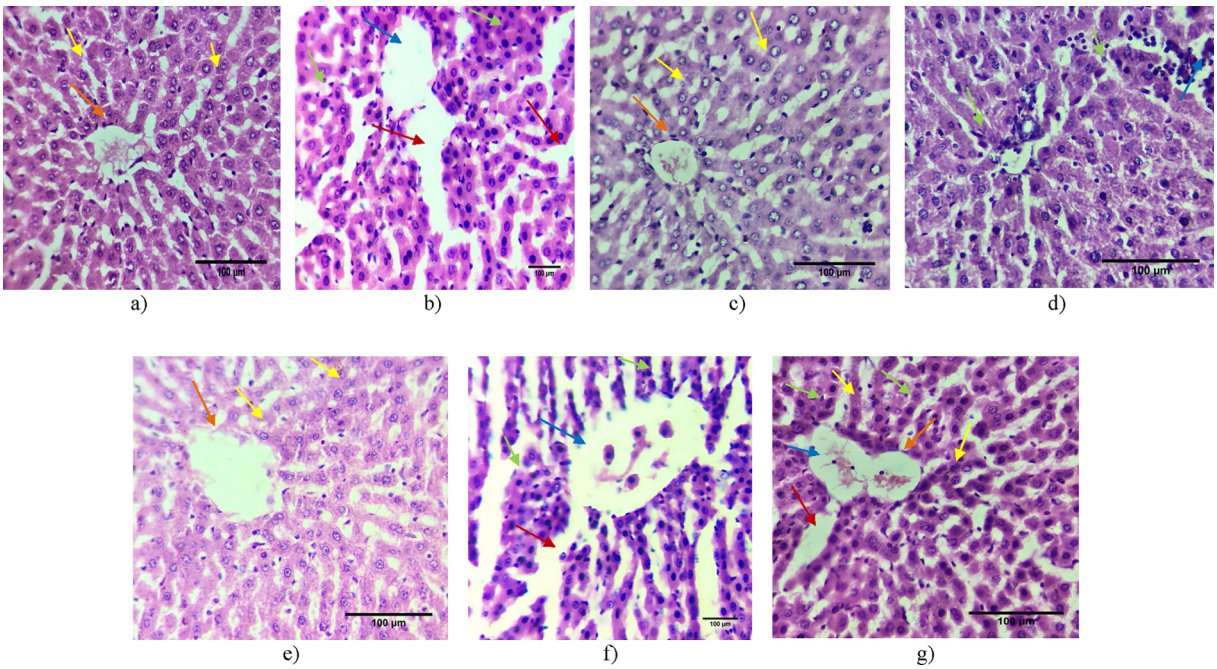

Fig. 12. Histology of the liver in experimental rats after 7 days of treatment (H&E, 400×). (a) Group I: normal animals showed hepatocytes (yellow arrow), central vein (orange arrow), (b) Group II: STZ + NA showed dilated and absence of nucleus in hepatocytes (green arrow), irregular and dilated central vein (blue arrow), vacuolization of cytoplasm (red arrow), (c) Group III: Metformin 100 mg/kg showed normal liver architecture, (d) Group IV: DCCU 15 mg/kg showed damage of liver cells, (e) Group V: DCCU 30 mg/kg reverted the hepatic damage, (f) Group VI: DCCT 15 mg/kg showed damage of liver cells, and (g) Group VII: DCCT 30 mg/kg showed partial protection of diabetic liver tissue. (For interpretation of the references to colour in this figure legend, the reader is referred to the web version of this article.)

insulin resistance. In addition, Rambabu et al. [100] stated that 3,4,5-trimethoxybenzohydrazide analogs having 3,4,5-trimethoxy substitution attached to the pyridine ring had important anti-diabetic activity compared to insulin.

STZ-induced diabetes induces oxidative stress, which was unregulated by naturally occurring antioxidants such as superoxide dismutase (SOD) and decreased glutathione (GSH) etc., contributing to disruption to essential compounds such as lipids, proteins and so on via

oxidation in animals [42]. Malondialdehyde (MDA) is a by-product of tissue degradation that shows the extent of lipid peroxidation. In this analysis, elevated MDA rates in animal pancreatic and liver tissue revealed reduced antioxidant protection and increased oxidative stress in diabetic rats. On the other side, we found a decline in antioxidant enzymes such as SOD and GSH in pancreatic and liver tissue of diabetes-induced rats (STZ + NA).

Superoxide dismutase and GSH can catalyze free radicals and hydrogen peroxide (which causes cell damage) into molecular oxygen. In the current study, *in vivo* anti-diabetic screening findings revealed that a significant rise in MDA level and a large decrease in SOD and GSH in pancreatic and liver tissue of STZ + NA induced diabetic rats relative to control rats. Further therapy with 30 mg/kg b.d. Doses of DCCU 13 (Group V) and DCCT 13 (Group VII) demonstrated a large and modest decrease in MDA and a rise in SOD and GSH rates in pancreatic and liver tissues of diabetic rats compared with diabetic animals treated with 100 mg/kg b.d. the normal dosage of Metformin. All these findings are consistent with the results stated by Perez-Gutierrez and co-workers [101,102] that treatment with coumarin-chalcone derivatives isolated from the *Eysenhardtia polystachya* bark significantly decreases the MDA level and significantly increases the SOD and GSH levels in the pancreas, liver, and kidneys of diabetic animals.

The histopathological observation of the pancreas isolated from diabetic animals visualizes shrunken, necrosis, and vacuolization of the cytoplasm of β-cells [103–107]. Current histopathological examination of pancreas tissue isolated from STZ + NA induced diabetic rats, exhibits β-islet cell shrunk, cell necrosis, and vacuolization of cytoplasm, further treatment with DCCU 13 (30 mg/kg) and Metformin (100 mg/kg) b.d. dose protected the β-islet cells. In fact, limited defense of pancreatic tissue injury was reported with DCCT 13 (30 mg/kg) b.d. therapy. Histopathological studies of liver tissue extracted from diabetic control group animals revealed dilated hepatocytes with no nucleus, abnormal and dilated central vein canal, increased vacuolation of hepatocyte cytoplasm [103,105–109]. In the same direction, the current histopathological analysis of the liver extracted from STZ + NA-induced diabetic rats visualizes dilated hepatocytes with no nucleus, abnormal and dilated central vein canal, increased vacuolization of hepatocyte cytoplasm, further treatment with 100 mg/kg b.d. dose of metformin promotes significant protection of damaged hepatocytes, degenerated, apoptotic and dilated sinusoidal veins, treatment with 30 mg/kg b.d. dose of DCCU 13 and DCCT 13 promotes partial protection of damaged hepatic architecture. Literature reports on STZ indicated that elevated ROS showed detrimental influence in hepatic cells and β-islet cell architecture, whereas treatment with coumarin analogs (3′,4′-Di-O-acetyl-*cis*-khellactone) mitigated the effect of STZ on β-islet and hepatic cells histology [110].

5. Conclusion

This research work describes the effective design, synthesis, and elucidation of anti-diabetic activity of new coumarin-chalcone hybrids through *in silico* and *in vivo* screening techniques. The synthesis of titled hybrids was done by well-known chemical reactions like Biginelli synthesis, Pechmann condensation, Acetylation, and Claisen-Schmidt reactions. The *in silico* docking results indicated that most of the compounds designed showed significant insulin receptor docking scores (PDB ID: 1IR3) indicating their strong affinity to target proteins, particularly DCCU 13 hybrids, and DCCT 13 showed more affinity in terms of target protein docking score compared to the internal ligand ANP and standard drug Metformin. The effective anti-diabetic hybrids identified through *in silico* studies against insulin protein were evaluated through *in vivo* anti-diabetic activity on STZ + NA induced diabetic rats. Results suggested that the hybrids exhibited potent and moderate anti-diabetic activity at a dose of 30 mg/kg by significantly reducing blood glucose levels, reducing weight loss, regulating oxidative stress and restoring degenerated β-islet cells. However, the enhancement of the mechanism of insulin resistance of these anti-diabetic agents can be elucidated by more selective procedures.

Declaration of Competing Interest

The authors declare that they have no known competing financial interests or personal relationships that could have appeared to influence the work reported in this paper.

Acknowledgments

The authors thank the University grant commission (UGC, New Delhi, India), Acahrya Nagarjuna University College of Pharmaceutical Sciences, Acharya Nagarjuna University, Guntur, A. P., India and VLife Technologies, Pune, India, for their support and encouragement.

References

[1] J.A. da Silva, E.C.F. de Souza, A.G.E. Boschemeier, C.C.M. da Costa, H.S. Bezerra, E.E.L.C. Feitosa, Diagnosis of diabetes mellitus and living with a chronic condition: participatory study, BMC Public Health 18 (2018) 1–8.
[2] American Diabetes Association, Diagnosis and classification of diabetes mellitus, Diabetes Care 32 (2009) S62–S67.
[3] A. Chawla, R. Chawla, S. Jaggi, Microvasular and macrovascular complications in diabetes mellitus: Distinct or continuum? Indian J. Endocrinol. Metab. 20 (2016) 546–551.
[4] A. Chaudhury, C. Duvoor, V.S.R. Dendi, Clinical review of antidiabetic drugs: implications for type 2 diabetes mellitus management, Front. Endocrinol. 8 (2017) 1–12.
[5] S. Wild, G. Roglic, A. Green, R. Sicree, H. King, Global prevalence of diabetes: estimates for the year 2000 and projections for 2030, Diabetes Care 27 (2004) 1047–1053.
[6] C. Viegas-Junior, A. Danuello, V. da Silva Bolzani, E.J. Barreiro, C.A. Fraga, Molecular hybridization: a useful tool in the design of new drug prototypes, Curr. Med. Chem. 14 (2007) 1829–1852.
[7] A. Le, T.C.Q. Phan, T.H. Nguyen, *In silico* drug design: Prospective for drug lead discovery, Int. J. Engi. Sci. Inven. 4 (2015) 60–70.
[8] N. Kerru, A. Singh-Pillay, P. Awolade, P. Singh, Current anti-diabetic agents and their molecular targets: A review, Eur. J. Med. Chem. 152 (2018) 436–488.
[9] O.R. Gottlieb, K.R.D.H. Herrmann Murray, G. Ohloff, G. Pattenden, Progress in the Chemistry of Organic Natural Products, Springer-Verlag Wein, 1978, p. 200.
[10] H.V. Pechmann, C. Duisberg, Chem. Tech. Ber. 17 (1884) 927.
[11] E. Knoevenagel, On the chemistry of the condensing action of ammonia and organic amines in reactions between aldehydes and acetoacetic ester, Ber. Dtsch. Chem. Ges. 31 (1898) 738–748.
[12] J.R. Johnson, Perkin Reaction and Related Reactions, Org. React. 1 (1942) 210–265.
[13] L. Bert, Compt. Rend. 214 (1942) 230.
[14] R.L. Shirner, Org. React. 1 (1942) 1.
[15] I. Yavari, R. Hekmat-shoar, A. Zonouzi, A new and efficient route to 4-carboxymethylcoumarins mediated by vinyl triphenyl phosphonium salt, Tetrahedron Lett. 39 (1998) 2391–2392.
[16] I. Manolov, N.D. Danchev, Synthesis, toxicological and pharmacological assessment of some 4-hydroxycoumarin derivatives, Eur. J. Med. Chem. Chim. Ther. 30 (1995) 531–536.
[17] D.A. Ostrov, J.A. Hernandez Prada, P.E. Corsino, K.A. Finton, N. Le, T.C. Rowe, Discovery of novel DNA gyrase inhibitors by high-throughput virtual screening, Antimicrob. Agents Chemother. 51 (2007) 3688–3698.
[18] K. Bhagat, J. Bhagat, M.K. Gupta, J.V. Singh, H.K. Gulati, A. Singh, K. Kaur, G. Kaur, S. Sharma, A. Rana, H. Singh, Design, synthesis, antimicrobial evaluation, and molecular modeling studies of novel indolinedione–coumarin molecular hybrids, ACS Omega 4 (5) (2019) 8720–8730.
[19] K.C. Fylaktakidou, D.J. Hadjipavlou-Litina, K.E. Litinas, D.N. Nicolaides, Natural and synthetic coumarin derivatives with anti-inflammatory/ antioxidant activities, Curr. Pharm. Des. 10 (2004) 3813–3833.
[20] Y. Bansal, P. Sethi, G. Bansal, Coumarin: a potential nucleus for anti-inflammatory molecules, Med. Chem. Res. 22 (2013) 3049–3060.
[21] M.E. Riveiro, A. Moglioni, R. Vazquez, N. Gomez, G. Facorro, L. Piehl, E.R. de Celis, C. Shayo, C. Davio, Structural insights into hydroxycoumarin-induced apoptosis in U-937 cells, Bioorg. Med. Chem. 16 (2008) 2665–2675.
[22] Y. Kashman, K.R. Gustafson, R.W. Fuller, J.H. Cardellina, J.B. McMahon, M.J. Currens, R.W. Buckheit, S.H. Hughes, G.M. Cragg, M.R. Boyd, The Calanolides, a Novel HIV-Inhibitory Class of Coumarin Derivatives from the Tropical Rainforest Tree, *Calophyllum lanigerum*, J. Med. Chem. 36 (1993) 1110.
[23] A. Manvar, A. Bavishi, A. Radadiya, J. Patel, V. Vora, N. Dodia, K. Rawal, A. Shah, Diversity oriented design of various hydrazides and their *in vitro* evaluation against Mycobacterium tuberculosis H37Rv strains, Bioorg. Med. Chem. Lett. 21 (2011) 4728–4731.
[24] J.Y. Yeh, M.S. Coumar, J.T. Horng, H.Y. Shiao, H.L. Lee, Anti-influenza drug discovery: structure-activity relationship and mechanistic insight into novel

angelicin derivatives, J Med. Chem. 53 (2010) 1519–1533.
[25] P. Anand, B. Singh, N. Singh, A review on coumarins as acetylcholinesterase inhibitors for Alzheimer's disease, Bioorg. Med. Chem. 20 (2012) 1175–1180.
[26] M. Curini, F. Epifano, F. Maltese, M.C. Marcotullio, S.P. Gonzales, J.C. Rodriguez, Synthesis of Collinin, an Antiviral Coumarin, Aust. J. Chem. 56 (2003) 59–60.
[27] B. Yuce, O. Danis, A. Ogan, G. Sener, M. Bulut, A. Yarat, Antioxidative and lipid lowering effects of 7,8-dihydroxy-3- (4-methylphenyl) coumarin in hyperlipidemic rats, Arzneim. Forsch. Drug Res. 59 (2009) 129–134.
[28] T. Namba, O. Morita, S.L. Huang, K. Goshima, M. Hattori, N. Kakiuchi, Studies on cardio-active crude drugs; I. Effect of coumarins on cultured myocardial cells, Planta Med. 54 (1988) 277–282.
[29] N.I. Baek, E.M. Ahn, H.Y. Kim, Y.D. Park, Furanocoumarins from the root of *Angelica dahurica*, Archiv. Pharm. Res. 23 (2000) 467–470.
[30] M.I. Yusupov, G.P. Sidyakin, Fraxidin and isofraxidin from *Artemisia scotina*, Chem. Natural Compd. 11 (1975) 94.
[31] M. Tinel, J. Belghiti, V. Descatoire, Inactivation of human liver cytochrome P-450 by the drug methoxsalen and other psoralen derivatives, Biochem. Pharmacol. 36 (1987) 951–955.
[32] C. Wang, A. Pei, J. Chen, A natural coumarin derivative esculetin offers neuroprotection on cerebral ischemia/reperfusion injury in mice, J. Neurochem. 121 (2012) 1007–1013.
[33] A.I. Khan, V.M. Kulkarni, M. Gopal, S.M. Shahabuddin, M.S. Chung, Synthesis and biological evaluation of novel angularly fused polycyclic coumarins, Bioorg. Med. Chem. Lett. 15 (2005) 3584–3587.
[34] W. Gajanan, A. Rahul, K. Neha, R. Ravi, K.K. Naveen, S. Dinkar, Synthesis of novel α-pyranochalcones and pyrazoline derivatives as Plasmodium falciparum growth inhibitors, Bioorg. Med. Chem. Lett. 20 (2010) 4675–4678.
[35] L. Xin-Hua, L. Jun, B.S. Jing, S. Bao-An, Q. Xing-Bao, Design and synthesis of novel 5-phenyl-N-piperidine ethanone containing 4,5-dihydropyrazole derivatives as potential antitumor agents, Eur. J. Med. Chem. 51 (2012) 294–299.
[36] H. Singh, J.V. Singh, M.K. Gupta, A.K. Saxena, S. Sharma, K. Nepali, P.M. Bedi, Triazole tethered isatin-coumarin based molecular hybrids as novel antitubulin agents: Design, synthesis, biological investigation and docking studies, Bioorg. Med. Chem. Lett. 27 (17) (2017) 3974–3979.
[37] H. Singh, M. Kumar, K. Nepali, M.K. Gupta, A.K. Saxena, S. Sharma, P.M. Bedi, Triazole tethered C5-curcuminoid-coumarin based molecular hybrids as novel antitubulin agents: Design, synthesis, biological investigation and docking studies, Eur. J. Med. Chem. 116 (2016) 102–115.
[38] C. Yin, W. Songlin, X. Xiangqing, L. Xin, Y. Minquan, Z. Song, L. Shicheng, Q. Yinli, Z. Tan, L. Bi-Feng, Z.J. Guisen, Synthesis and Biological Investigation of Coumarin Piperazine (Piperidine) Derivatives as Potential Multireceptor Atypical Antipsychotics, Med. Chem. 56 (2013) 4671–4690.
[39] H. Singh, J.V. Singh, K. Bhagat, H.K. Gulati, M. Sanduja, N. Kumar, N. Kinarivala, S. Sharma, Rational approaches, design strategies, structure activity relationship and mechanistic insights for therapeutic coumarin hybrids, Bioorg. Med. Chem. 27 (16) (2019) 3477–3510.
[40] T. Gireesh, R.K. Ravindra, P.K. Pramod, B.K. Sheetal, Synthesis of 3-aryl-4-({2-[4-(6-substituted-coumarin-3-yl)-1,3-thiazol-2-yl]hydrazinylidene}methyl/ethyl)-sydnones using silica sulfuric acid and their antidiabetic, DNA cleavage activity, Arab. J. Chem. 9 (2016) S306–S312.
[41] H.K. Gulati, K. Bhagat, A. Singh, N. Kumar, A. Kaur, A. Sharma, S. Heer, H. Singh, J.V. Singh, P.M. Bedi, Design, synthesis and biological evaluation of novel indolinedione–coumarin hybrids as xanthine oxidase inhibitors, Med. Chem. Res. (2020) 1–1.
[42] X. Chen, R. Pi, Y. Zou, Attenuation of experimental autoimmune encephalomyelitis in C57 BL/6 mice by osthole, a natural coumarin, Eur. J. Pharmacol. 629 (2010) 40–46.
[43] G. Di Carlo, N. Mascolo, A.A. Izzo, F. Capasso, Flavonoids: old and new aspects of a class of natural therapeutic drugs, Life Sci. 65 (1999) 337–353.
[44] B. Orlikova, D. Tasdemir, F. Golais, M. Dicato, M. Diederich, Dietary chalcones with chemopreventive and chemotherapeutic potential, Genes. Nutr. 6 (2011) 125–147.
[45] A. Guida, M.H. Lhouty, D. Tichit, F. Figueras, P. Geneste, Hydrotalcites as base catalysts. Kinetics of Claisen-Schmidt condensation, intramolecular condensation of acetonylacetone and synthesis of chalcone, Appl. Catal. A 164 (1997) 251.
[46] N. Eddarir, S. Catelle, Y. Bakkour, C. Ronlando, An efficient synthesis of chalcones based on the Suzuki reaction, Tetrahedron Lett. 44 (2003) 5359–5363.
[47] A. Bohm, Introduction to Flavonoids, Harwood Academic Pub, London, 1998.
[48] K. Fukui, T. Matsumoto, S. Nakamura, M. Nakayama, Synthetic studies of the flavone derivatives. VII. The synthesis of jaceidin, Bull. Chem. Soc. Jpn. 41 (1968) 1413–1417.
[49] M. Al-Masum, E. Ng, M. Wai, Palladium-catalyzed direct cross-coupling of potassium styryltrifluoroborates and benzoyl chlorides—a onestep method for chalcone synthesis, Tetrahedron Lett. 52 (2011) 1008–1010.
[50] Y.K. Srivastava, Ecofriendly microwave assisted synthesis of Some chalcones, Ras. J. Chem. 1 (2008) 884–886.
[51] A. Kumar, S. Sharma, V.D. Tripathi, S. Srivastava, Synthesis of chalcones and flavanones using Julia-Kocienski olefination, Tetrahedron 66 (2010) 9445–9449.
[52] S. Zangade, S. Mokle, A. Vibhute, Y. Vibhute, An efficient and operationally simple synthesis of some new chalcones by using grinding technique, Chem. Sci. J. CSJ13 (2011) 1–5.
[53] G.B. Bagihalli, P.G. Avaji, S.A. Patil, P.S. Badami, Synthesis, spectral characterization, *in vitro* antibacterial, antifungal and cytotoxic activities of Co (II), Ni (II) and Cu (II) complexes with 1, 2, 4-triazole Schiff bases, Eur. J. Med. Chem. 43 (12) (2008) 2639–2649.
[54] D.S. Satyajit, N. Lutfun, Chemistry for Pharmacy Students General, Organic and Natural Product Chemistry, The Atrium, Southern Gate, Chichester, West Sussex, England, 2007.
[55] J. Portugal, Chartreusin, elsamicin A and related anti-cancer antibiotics, Curr. Med. Chem.-Anti-Cancer Agents 3 (6) (2003) 411–420.
[56] Y. Kashman, K.R. Gustafson, R.W. Fuller, HIV inhibitory natural products. Part 7. The calanolides, a novel HIV-inhibitory class of coumarin derivatives from the tropical rainforest tree, Calophyllum lanigerum, J. Med. Chem. 35 (1992) 2735–2743.
[57] S.H. Kim, K.A. Kang, R. Zhang, Protective effect of esculetin against oxidative stress-induced cell damage via scavenging reactive oxygen species, Acta Pharmacol. Sin. 29 (2008) 1319–1326.
[58] J. Hirsh, J.E. Dalen, D.R. Anderson, Oral anticoagulants: mechanism of action, clinical effectiveness, and optimal therapeutic range, Chest 119 (2001) 8S–21S.
[59] C.C. Chiang, M.J. Cheng, C.F. Peng, H.Y. Huang, I.S. Chen, A novel dimeric coumarin analog and antimycobacterial constituents from Fatoua pilosa, Chem. Biodivers. 7 (2010) 1728–1736.
[60] C. Gopi, V.G. Sastry, M.D. Dhanaraju, Design, synthesis, spectroscopic characterization and anti-psychotic investigation of some novel Azo dye/Schiff base/Chalcone derivatives, Egypt. J. Basic Appl. Sci. 4 (4) (2017) 270–287.
[61] P. Geetha, N. Pramod, B. Mahaboob, M. Deepa, P. Neelaphar, B.H.M. Jayakumar Swamy, Design, synthesis and anti-malarial activity of coumarin fused quinoline derivatives, J. Pharm. Res. 10 (2016) 437–441.
[62] T. Moodley, M. Momin, C. Mocktar, C. Kannigadua, N.A. Koorbanally, The synthesis, structural elucidation and antimicrobial activity of 2- and 4-substituted-coumarinyl chalcones, Magn. Reson. Chem. 54 (2016) 610–617.
[63] S. Vazquez-Rodriguez, R.L. Lopez, M.J. Matos, G. Armesto-Quintas, S. Serra, E. Uriarte, L. Santana, F. Borges, A.M. Crego, Y. Santos, Design, synthesis and antibacterial study of new potent and selective coumarin–chalcone derivatives for the treatment of tenacibaculosis, Bioorg. Med. Chem. 23 (2015) 7045–7052.
[64] K.V. Sashidhara, A. Kumar, M. Kumar, J. Sarkar, S. Sinha, Synthesis and *in vitro* evaluation of novel coumarin-chalcone hybrids as potential anticancer agents, Bioorg. Med. Chem. Lett. 20 (2010) 7205.
[65] S. Valente, E. Bana, E. Viry, D. Bagrel, G. Kirsch, Synthesis and biological evaluation of novel coumarin-based inhibitors of Cdc25 phosphatases, Bioorg. Med. Chem. Lett. 20 (2010) 5827.
[66] K. Patel, C. Karthikeyan, N.S. Hari Narayana Moorthy, S.D. Girdhar, R.S. Viswas, L. Hoyun, T. Piyush, Design, synthesis and biological evaluation of some novel 3-cinnamoyl-4-hydroxy-2H-chromen-2-ones as antimalarial agents, Med. Chem. Res. 21 (2011) 1780.
[67] G. Wanare, R. Aher, N. Kawathekar, R. Ranjan, N.K. Kaushik, D. Sahal, Synthesis of novel alpha-pyranochalcones and pyrazoline derivatives as Plasmodium falciparum growth inhibitors, Bioorg. Med. Chem. Lett. 20 (2010) 4675.
[68] X. Gao-Lei, L. Zai-Qun, Coumarin moiety can enhance abilities of chalcones to inhibit DNA oxidation and to scavenge radicals, Tetrahedron 70 (2014) 8397.
[69] F. Perez-Cruz, S. Vazquez-Rodriguez, M. Joao Matos, A. Herrera-Morales, A.V. Frederick, A. Das, G. Bhavani, C. Olea-Azar, S. Lourdes, U. Eugenio, Synthesis and electrochemical and biological studies of novel coumarin-chalcone hybrid compounds, J. Med. Chem. 56 (2013) 6136.
[70] I. Ahmad, J.P. Thakur, D. Chanda, D. Saikia, F. Khan, S. Dixit, A. Kumar, R. Konwar, A.S. Negi, A. Gupta, Syntheses of lipophilic chalcones and their conformationally restricted analogues as antitubercular agents, Bioorg. Med. Chem. Lett. 23 (2013) 1322.
[71] D.K. Yadav, I. Ahmad, A. Shukla, K. Feroz, N. Aravid, G. Atul, QSAR and docking studies on chalcone derivatives for antitubercular activity against M. tuberculosis H37Rv, J. Chemometr. 28 (2014) 499.
[72] B.S. Jayashree, Y. Shakkeela, D. Vijay Kumar, Synthesis of some coumarinyl chalcones of pharmacological interest, Asian J. Chem. 21 (2009) 5918.
[73] T.H.H. Tawassl, A.E.M. Saeed, Green chemistry approach in synthesis of 3,4-dihydropyrimidinone derivatives under solvent-free conditions, Int. J. Pharm. Sci. Res. 6 (2015) 2191–2197.
[74] C.T. Jalpa, B.B. Jitender, D.U. Kuldip, T.N. Yogesh, K.J. Sudhir, C.P. Christophe, D.C. Erik, K.S. Anamik, Improved and rapid synthesis of new coumarinyl chalcone derivatives and their antiviral activity, Tetrahedron Lett. 48 (2007) 8472–8478.
[75] V.N. Dholakia, M.G. Parekh, K.N. Trivedi, Studies in 4-hydroxy coumarins. II. α- and γ-Pyrones from 4-hydroxy coumarins, Aust. J. Chem. 21 (1968) 2345–2347.
[76] Y.R. Prasad, A.L. Rao, R. Rambabu, Synthesis and antimicrobial activity of some chalcone derivatives, E-J. Chem. 5 (2008) 461–469.
[77] OECD/OCDE, OECD guideline for testing of chemicals: Acute Oral Toxicity – Acute Toxic Class Method 423 (2001).
[78] H.R. Madkor, S.W. Mansour, G. Ramadan, Modulatory effects of garlic, ginger, turmeric and their mixture on hyperglycaemia, dyslipidaemia and oxidative stress in streptozotocin-nicotinamide diabetic rats, Br. J. Nutr. 105 (2011) 1210–1217.
[79] K. Pawan, L.K. Sukhbir, A.C. Rana, K. Dhirender, Pharmacophore modeling and molecular docking studies on pinus roxburghii as a target for diabetes mellitus, Adv. Bioinf. (2014) 1–8.
[80] S.L. Marklund, G. Marklund, Involvement of the superoxide anion radical in the autoxidation of pyrogallol and a convenient assay for superoxide dismutase, Eur. J. Biochem. 47 (1974) 469.
[81] N.O. Soni, Antioxidant assay *in vivo* and *in vitro*, Int. J. Phytopharmacol. 5 (2014) 51–58.
[82] I. Rahman, A. Kode, S.K. Biswas, Assay for quantitative determination of glutathione and glutathione disulfide levels using enzymatic recycling method, Nat. Protoc. 1 (2007) 3159–3165.
[83] S.I. Rizvi, M.A. Zaid, Intracellular reduced glutathione content in normal and type 2 diabetic erythrocytes: Effect of insulin and (-)epicatechin, J. Physiol. Pharmacol. 52 (2001) 483–488.

[84] E. Ramu, V. Kotra, N. Bansal, R. Varala, S.R. Adapa, Green approach for the efficient synthesis of Biginelli compounds promoted by citric acid under solvent-free conditions, RAS AYAN J. Chem. 1 (1) (2008) 188–194.
[85] S. Sethna, R. Phadke, The Pechmann reaction, Org. React. 7 (2004) 1–58.
[86] P. Strugala, O. Dzydzan, I. Brodyak, Antidiabetic and Antioxidative potential of the blue congo variety of purple potato extract in streptozotocin-induced diabetic rats, Molecules 24 (2019) 1–22.
[87] M. Vineet, S. Arun, K. Pallavi, M. Udayabanu, Antioxidant, anti-inflammatory, and antidiabetic activity of hydroalcoholic extract of ocimum sanctum: an *in-vitro* and in-silico study, Asian J. Pharm. Clin. Res. 9 (2016) 44–49.
[88] K. Manokaran, A. Ramasamy, B. Veluswamy, Molecular docking of compounds elucidated from Ixora coccinea Linn. flowers with insulin receptors, Der Pharmacia Lettre 7 (2015) 344–348.
[89] K. Tharini, K. Sundaresan, In-silico docking studies of anti-diabetic and breast cancer activity by n'-(1-benzylpiperidin-4-ylidene)-2-cyanoacetohydrazide, Int. J. of Adv. Res. 5 (2017) 601–607.
[90] S. Jeyabaskar, T. Viswanathan, R. Mahendran, M. Nishandhini, In-silico Molecular Docking studies to investigate interactions of natural Camptothecin molecule with diabetic enzymes, Res. J. Pharm. Tech. 10 (2017) 2917–2922.
[91] M. Priya, R.J. Caroline, Molecular docking studies of wattakaka volubilis flavonids as insulin receptor tyrosin kinase activator as cure for diabetes mellitus, Pharmacophore 5 (2014) 509–516.
[92] R.P. John, S.M. Sneha, S.V. Karthikeya, P. Anitha, B.P. Ravindra, Chromatographic analysis of phytochemicals in Costus igneus and computational studies of flavonoids, Inf. Med. Unlocked 13 (2018) 34–40.
[93] K. Sundaresan, K. Tharini, Synthesis, characterization and molecular level interaction study of insulin receptor with some cyanoacetyl hydrazone derivatives as a potent antidiabetic study, Int. J. Pharma. Res. Health Sci. 6 (2018) 2604–2609.
[94] S. Gurudeeban, K. Satyavani, T. Ramanathan, Effect of dichloromethane fraction of Rhizophora mucronata on carbohydrate, lipid and protein metabolism in type 2 diabetic rats, Integr. Obesity Diabetes 3 (2017) 1–8.
[95] J. Ganugapati, S. Swarna, Molecular docking studies of antidiabetic activity of cinnamon compounds, Asian J. Pharm. Clin. Res. 7 (2014) 31–34.
[96] N. Kaushik, N. Kumar, A. Kumar, Synthesis, antioxidant and antidiabetic of 1-[(5-sunstituted phenyl)-4,5-dihydro-1H-pyrazol-3-yl]-5-phenyl-2H-tetrazole, Indian J. Pharmaceut. Sci. 78 (2006) 352–359.
[97] P.A. Datar, S.B. Aher, Design and synthesis of novel thiazolidine-2,4-dione as hypoglycaemic agents, J. Saudi Chem. Soc. (2016) 196–210.
[98] S. Prachand, A.K. Gupta, R. Gilhotra, Synthesis and biological activity of some novel imadazolidine analogues as potent antidiabetic activity, Int. J. Pharm. Sci. Res. 9 (2017) 2287–2292.
[99] S. Sucheta, P.K. Tahlan, Veerma, Synthesis, SAR and *in vitro* therapeutic potentials of thiazolidine-2,4-diones, Chem. Cent. J. 12 (2018) 129.
[100] N. Rambabu, B. Ram, P.K. Dubey, Synthesis and biological activity of novel (E)-N-(substituted)-3,4,5-trimethoxybenzohydrazide analogues, Orient. J. Chem. 33 (2017) 226–234.
[101] R. Singh, P. Bhardwaj, P. Sharma, Antioxidant and toxicological evaluation of Cassia sopherain streptozotocin-induced diabetic Wistar rats, Pharmacogn. Res. 5 (4) (2013) 225.
[102] R.M. Perez-Gutierrez, A.H. Garcia-Campoy, A. Muñiz-Ramirez, Properties of flavonoids isolated from the bark of Eysenhardtia polystachya and their effect on oxidative stress in streptozotocin-induced diabetes mellitus in mice, Oxidat. Med. Cell. Longevity (2016) 1–13.
[103] A. Rathinam, L. Pari, R. Chandramohan, B.A. Sheikh, Histopathological findings of the pancreas, liver, and carbohydrate metabolizing enzymes in STZ-induced diabetic rats improved by administration of myrtenal, J. Physiol. Biochem. 70 (4) (2014) 935–946.
[104] D.A. Almalki, S.A. Alghamdi, A.M. Al-Attar, Comparative study on the influence of some medicinal plants on diabetes induced by streptozotocin in male rats, Biomed Res. Int. 2019 (2019).
[105] D. Ahmed, M.I. Khan, G. Kaithwas, S. Roy, S. Gautam, M. Singh, U. Devi, R. Yadav, J. Rawat, S. Saraf, Molecular docking analysis and antidiabetic activity of rifabutin against STZ-NA induced diabetes in albino wistar rats, Beni-Suef Univ. J. Basic Appl. Sci. 6 (3) (2017) 269–284.
[106] S. Yasmin, F. Capone, A. Laghezza, F. Dal Piaz, F. Loiodice, V. Vijayan, V. Devadasan, S.K. Mondal, Ö. Atlı, M. Baysal, A.K. Pattnaik, Novel benzylidene thiazolidinedione derivatives as partial PPARγ agonists and their antidiabetic effects on Type 2 diabetes, Sci. Rep. 7 (1) (2017) 1–7.
[107] A.S. Vinagre, A.D. Ronnau, S.F. Pereira, L.U. Silveira, E.D. Wiilland, E.S. Suyenaga, Anti-diabetic effects of Campomanesia xanthocarpa (Berg) leaf decoction, Brazil. J. Pharm. Sci. 46 (2) (2010) 169–177.
[108] N.M. Elamin, I.M. Fadlalla, S.A. Omer, H.A. Ibrahim, Histopathological alteration in STZ-nicotinamide diabetic rats, a complication of diabetes or a toxicity of STZ, Int. J. Diabetes Clin. Res. 5 (2018) 091.
[109] Q. Ma, Y. Guo, L. Sun, Y. Zhuang, Anti-diabetic effects of phenolic extract from rambutan peels (Nephelium lappaceum) in high-fat diet and streptozotocin-induced diabetic mice, Nutrients 9 (8) (2017) 801.
[110] E.A. Dominguez-Mendoza, J. Cornejo-Garrido, E. Burgueño-Tapia, C. Ordaz-Pichardo, Antidiabetic effect, antioxidant activity, and toxicity of 3′, 4′-Di-O-acetyl-cis-khellactone in Streptozotocin-induced diabetic rats, Bioorg. Med. Chem. Lett. 26 (16) (2016) 4086–4091.